creative commons
COMMONS DEED

저작자표시-비영리-변경금지 2.0 대한민국

이용자는 아래의 조건을 따르는 경우에 한하여 자유롭게

- 이 저작물을 복제, 배포, 전송, 전시, 공연 및 방송할 수 있습니다.

다음과 같은 조건을 따라야 합니다:

저작자표시. 귀하는 원저작자를 표시하여야 합니다.

비영리. 귀하는 이 저작물을 영리 목적으로 이용할 수 없습니다.

변경금지. 귀하는 이 저작물을 개작, 변형 또는 가공할 수 없습니다.

- 귀하는, 이 저작물의 재이용이나 배포의 경우, 이 저작물에 적용된 이용허락조건을 명확하게 나타내어야 합니다.
- 저작권자로부터 별도의 허가를 받으면 이러한 조건들은 적용되지 않습니다.

저작권법에 따른 이용자의 권리는 위의 내용에 의하여 영향을 받지 않습니다.

이것은 이용허락규약(Legal Code)을 이해하기 쉽게 요약한 것입니다.

Disclaimer

dCollection

A Dissertation
for the Degree of Doctor of Philosophy

Studies on the development of biomimetic microenvironment for stem cell culture

줄기세포 배양에 적합한 생체모사 배양미세환경 개발 연구

June, 2018

By

Myungook Lee

Department of Agricultural Biotechnology
Graduate School, Seoul National University

Studies on the development of biomimetic microenvironment for stem cell culture

줄기세포 배양에 적합한 생체모사 배양미세환경 개발 연구

지도교수 임 정 묵

이 논문을 농학박사 학위논문으로 제출함
2018년 6월

서울대학교 대학원
농생명공학부 바이오모듈레이션 전공

이 명 욱

이명욱의 박사학위논문을 인준함
2018년 7월

위 원 장 _____ (인)

부위원장 _____ (인)

위 원 _____ (인)

위 원 _____ (인)

위 원 _____ (인)

SUMMARY

This research describes the development of a three-dimensional (3D) system for *in vitro* culture of mouse embryonic stem cells (mESCs) and human adipose-derived stromal cells (hADSCs) in a biomimetic, non-cellular microenvironment.

Because it was assumed that each type of stem cell requires its own customized microenvironment in a biomimetic culture system, a 3D microenvironment was developed for mESCs and hADSCs, and the results were compared.

First, a method to isolate and analyze high quality oocytes from young and aged mice was developed. Second, integrin expression on the surface of inbred R1 and hybrid B6D2F1 mouse ESCs were screened to analyze cell-to-cell extracellular matrix (ECM) interactions before constructing a biomimetic microenvironment. After functional analysis of integrin heterodimers, we confirmed that the integrin heterodimers $\alpha_6\beta_1$ and $\alpha_v\beta_1$ actively functioned on the surface of undifferentiated mESCs of both strains. For the next step, to construct a biomimetic microenvironment customized for self-renewal and proliferation of mESCs, we evaluated whether different types of mESCs needed different types of 3D synthetic scaffolds for cell self-renewal. In

this step, the mechanical strength of microenvironments were varied, illustrating that different mESCs required different cellular interactions in the microenvironment, which indicated that each cell line required customization of the mechanical properties of the microenvironment.

For hADSCs, similar but slightly different processes were performed. The hADSCs were isolated from adipose tissue and stabilized through culture processes and magnetic-activated cell sorting. Transcriptional and translational analyses showed that hADSCs expressed α_5, α_v, and β_1 subunits when under conventional culture methods. This result indicated that different combinations of integrin heterodimers were needed to create different 3D culture conditions for hADSCs when compared with those needed for mESCs. As a result, the suitable mechanical strength of microenvironments for hADSCs were different from those needed for the mESC cell lines.

Every cell line therefore needed a different biomimetic microenvironment for optimal culture. Overall, the establishment of a stabilized biomimetic microenvironmental culture system for stem cells will enable the development of *in vitro* biomimetics, which will help facilitate the development of clinical stem cell studies to develop novel therapies.

Key Words: Embryonic stem cells, Adipose-derived stromal cells, Integrin, adhesion peptide, three-dimensional biomimetic microenvironment, polyethylene glycol-based hydrogel

Student number 2010-24124

CONTENTS

LIST OF FIGURES

LIST OF TABLES

LIST OF ABBREVIATIONS

2D	: two-dimensional
3D	: three-dimensional
ADSC	: adipose-derived stromal cells
ANOVA	: analysis of variance
DMEM	: Dulbecco's modified eagle's medium
FBS	: fetal bovine serum
ECM	: extracellular matrix
ESC	: embryonic stem cells
ICM	: inner cell mass
LIF	: leukemia inhibitory factor
MEF	: mouse embryonic fibroblast
MMP	: matrix metalloproteinases
PEG	: polyethylene glycol
VS	: vinylsulfone

CHAPTER 1

: General Introduction

Stem cells are undifferentiated cells that are able to differentiate into specialized cell types. The main characteristics of stem cells are their self-renewal capabilities and their ability to differentiate. Stem cells are a source of specialized cells that make up living tissues and organs of animals and plants. Because of these characteristics, stem cells have the potential to be used in the development of therapies for cell replacement, organ regeneration, and a variety of disorders and injuries, such as Parkinson's disease, heart disease, and other serious disorders. (Parekkadan and Milwid, 2010, Park et al., 2008)

There are two major types of stem cells: ESCs and adult stem cells (ASCs). ESCs are stem cells that are derived from the inner cell mass of blastocysts. Pluripotency is a unique characteristic of ESCs. They can differentiate into a variety of cell types that include all three embryonic germ layers. (Thomson et al., 1998). ASCs, which are also called somatic stem cells, are generally isolated from several types of adult tissues or organs, such as the umbilical cord, bone marrow, adipose tissue, and other tissues. ASCs exist throughout the body after embryonic development, and maintain and repair the tissue in which they are located. (Wagner et al., 2005, Kern et al., 2006)

To establish stem cells in the laboratory, they are isolated

from embryos or adult tissues and placed in a culture dish. After isolation, the cells are cultured in a controlled environment that inhibits uncontrolled differentiation but allows them to replicate. When stem cells are allowed to continuously self-renew under controlled culture conditions in a homozygous state, they become a stem cell line. (Thomson et al., 1998)

mESCs, which were first reported in 1981, are the most highly studied type of stem cells.(Evans and Kaufman, 1981) mESCs are widely used as a preclinical model for cell therapy and to develop genetically modified mice. Unfortunately, one of the major problems in the establishment of mESCs involves limited sources of ESCs. Although numerous oogonia, which are ESC progenitor cells, exist in mammalian ovaries as precursor cells, less than 1% of them are ovulated from the ovaries throughout the life of the organism.(McGee and Hsueh, 2000) Most oocyte precursor cells in the ovaries degenerate; thus, the total number of oocytes produced in mammalian ovaries is limited. Many previous studies have used young mice as oocyte donors because large numbers of oocytes are ovulated from young animals.(Lee et al., 2008) However, if the experimental mice are older, it is difficult to obtain a sufficient number of oocytes, and the developmental competence of these oocytes is relatively low. This makes it difficult to conduct

studies that involve breeding or obtaining experimental results. In the present study, based on the aforementioned difficulties, superovulation methods were optimized to obtain large numbers of quality oocytes from young and aged mice.

Mesenchymal stromal cells or mesenchymal stem cells (MSCs) are a type of ASC that are isolated from bone marrow, cord cells, amniotic fluid, and adipose tissue.(Fraser et al., 2007, Hass et al., 2011) Because of their self-renewal potential, pluripotency, and immune privilege, MSCs can potentially be used to develop clinical cell therapies for degenerative diseases. (Sensebe et al., 2010, Mariani and Facchini, 2012)

The most widely used system in cell culture involves cell growth on a two-dimensional (2D) surface. Although this traditional 2D cell culture method provides a well-defined system, its structural differences compared with *in vivo* systems have been extensively recognized. Every *in vivo* stem cell is surrounded by ECM and other cells in a 3D arrangement, which is very different from traditional 2D culture systems. In 2D culture systems, cells come into contact with other cells only at their edges, with most of their surface in contact with plastic, and only one surface in contact with ECM. Under these 2D culture conditions, the cells may behave differently than if they were in an *in vivo* 3D environment.(Duval et

al., 2017)

A 3D culture system representing the actual *in vivo* 3D microenvironment of cells has recently been developed. Cells in 3D culture exhibit different morphology and physiology from cells in traditional 2D culture. A polyethylene glycol (PEG)-based 3D culture can be generated by dispersing cells in a liquid matrix, followed by polymerization. This PEG-based 3D culture allows cells to grow naturally in a 3D environment, with cell-ECM interactions occurring in 360°. However, limited cell growth has been reported in past studies of 3D cultures. (Lei and Schaffer, 2013) In the present study, we developed various 3D culture systems to determine the optimal conditions for 3D cell growth.

Various types and large quantities of ESCs are needed for both basic research and clinical use. To obtain large quantities of ESCs, it is necessary to collect large numbers of oocytes before establishing ESCs. The optimal method of superovulation could result in the collection of a large number of oocytes. In addition, a hormonal effect was analyzed in both young and old mice to utilize the oocyte-collecting infrastructure in young and old mice. In Chapter 3, various superovulation methods were optimized to collect large numbers of oocytes. The hormonal effects of different types of gonadotropins in mice were analyzed, and the identification

of the developmental competence of oocytes was optimized depending on hormones and the age of the mice. Direct comparisons between 6-8-week-old mice and 45-65-week-old mice were then conducted after the superovulation treatments.

Artificial synthetic scaffolds were considered as a cellular niche in the construction of a 3D culture system. This cellular niche required three kinds of characteristics: geometric, biochemical, and mechanical properties. Geometric properties include the shape, porosity, and topography. Artificial synthetic scaffolds for cell culture should provide suitable form to support cells and should be easy to manipulate. In the present study, matrix metalloproteinase (MMP)-sensitive PEG-based hydrogel material was used as a synthetic scaffold. The PEG hydrogel allowed independent control of the physical characteristics of the scaffold. It contained MMP-sensitive peptides that allowed cell-mediated proteolytic matrix degradation and remodeling, which facilitated easy control of geometric and mechanical properties. (Lutolf and Hubbell, 2003) In Chapters 4 and 5, suitable conditions for artificial scaffolds in culturing mESCs were investigated. Integrin expression was first identified, to characterize interactions between mESCs and between cells and ECM. Moreover, various conditions of the PEG hydrogel were tested to maximize cell proliferation activity. The

identification of stemness-related activity was performed after culturing cells in artificial scaffolds, to confirm the cellular reactivity of mESCs in 3D culture. Previous studies in this laboratory showed that typical mESCs showed phenotypic changes in synthetic microenvironments optimized for culturing other types of mESCs. To confirm these differences, two different types of mESCs were employed as experimental cell lines. (Lee et al., 2016).

To test the clinical feasibility of 3D culture systems, it was necessary to evaluate human cell culture systems. In Chapter 6, hADSCs were employed as an experimental cell line to develop a hADSC-customized 3D culture system. Integrin expression in hADSCs was analyzed to identify cell-ECM interactions and to determine the best parameters for creating artificial scaffolds, and adhesion peptides were investigated to maximize cell proliferation. Based on these considerations, direct comparison of suitable culture conditions between hADSCs and mESCs could be made.

CHAPTER 2

: Literature Review

1. Embryonic stem cells

Embryonic stem cells (ESCs) are derived from inner cell mass of blastocyst which is and embryo before the implantation process. ESCs are expected as a promising cell source for cell therapies and basic research with following characteristics. First, ESCs could proliferate for a prolonged period of time with undifferentiated state. Second, ESCs could differentiate into all three types of embryonic germ layers even after being grown for a long time *in vitro.* Third, ESCs express large amount of stemness-related genes so it is easy to confirm the state of ESCs in research procedure (Hoffman and Carpenter, 2005).

Pluripotency is a fascinating point of ESCs and still remain unclear about their whole process. Oct4 is regarded as a key markers for ESCs and sufficient expression of Oct4 must be maintained in critical level to remain in undifferentiated state (Niwa et al., 2000). Moreover, this pluripotent properties are currently evaluated by a set of markers with Oct4, such as SSEA-1, 3, 4, TRA-1-60, and TRA-1-81 are generally used to characterize ESCs (Li et al., 2010).

Mouse ESCs and human ESCs were both conventionally grown on a feeder cell layer of mouse embryonic fibroblasts with serum. However, the factors that maintain the pluripotency of both cell types were still unclear. Leukemia inhibitory factor (LIF) is known as a key cytokine to sustain undifferentiated state of mouse

ESCs. LIF is known to modulate STAT3 pathway and also a critical factors to maintain undifferentiated state of mouse ESCs in conventional 2D culture systems. However, exact correlation about LIF and serum and feeder layer in mouse ESC culture is not clearly elucidated(Ying et al., 2003).

ESCs are promising cell source for treatments in tissue engineering and cell therapies for incurable diseases such as Parkinson's or diabetes (Fadini et al., 2017, Kingwell, 2013). However, there are still significant technical problems stand in the way of developing these treatments. Most pressing challenge is a cell loss and simultaneous differentiation of ESCs in treatment process. In laboratory research, the use of cultural scaffolds has contributed to a one of cell career and differentiation agents (Feng et al., 2011, Handschel et al., 2011, Sabaghi et al., 2016).

1.1 Establishment of ESCs

First Establishment of murine ESCs was performed at early 1980s (Evans and Kaufman, 1981, Martin, 1981). At early 1980s, isolation efficiency of mouse ESCs were very low and most of ESCs have been obtained from limited mouse strains (Evans and Kaufman, 1981, Martin, 1981). To improve establishment efficacy, many attempt have been tried to stable establishment of mouse ESCs. Use of mouse embryonic fibroblsts as feeder layer (Wobus et al., 1984), genetically modified mouse , mechanically modified

blastocyst (McWhir et al., 1996). The most major procedure for mouse ESC establishment protocol is reported by Bryja et al (Bryja et al., 2006). This protocol used inactivated feeder cells, Leukemia inhibitory factor (LIF), with serum replacement.

1.2 Collection of ESCs: Superovulation of oocyte

A large number of high quality oocytes was important in establishment of ESCs. There are standardized methods for ovarian superovulation and oocytes collection procedures studied by the previous researches. (Ertzeid and Storeng, 2001b)

The procedure for superovulation of oocytes involves hormonal treatments designed to induce follicular development and oocyte release. ((Brooke et al., 2007) The types of hormones used in inducing follicular development procedure were follicular stimulating hormone (FSH), human menopausal gonadotropin (HMG), or pregnant mare's serum gonadotropin (PMSG). The hormones used to release oocytes were luteinizing hormone (LH) and human chorionic gonadotropin (hCG). Other types of alternative hormones also have been reported successful superovulation results in mice, such as LH-releasing hormone analogue, or fertirelin acetate. (Nariai et al., 2005).

1.3 Characterization of ESCs

ESCs which have pluripotency always has capacity to differentiate into all three types of germ layers. To confirm pluripotency of ESCs, two characteristics of ESCs were mainly tested, stemness-related marker and differentiation potential. For stemness-related marker, number of genes were tested to examine undifferentiated state of ESCs. Oct4 (Scholer et al., 1990), Nanog (Chambers et al., 2003), Sox2 (Avilion et al., 2003), FGF4(Ginis et al., 2004), SSEA-1(Solter and Knowles, 1978), CD133 (Kania et al., 2005), CD9 (Oka et al., 2002), TRA-1-60, and TRA-1-81 (Li et al., 2010)...
To identify differentiation potential of ESCs, ESCs were cultured without LIF and feeder layer at suspension state (Keller, 1995). Then ESCs formed spherical structures called embryoid bodies (EB). After culturing EB for few days, three germ layer will appear if ESCs have pluripotency (Leahy et al., 1999). Other ways to confirm pluripotency is cell transplantation method and generate chimeric mice. When pluripotent ESCs were transplanted into immune deficient mice, ESC will transformed into teratomas which consist of all three germ layers differentiated from transplanted ESCs (Przyborski, 2005). The other method is generate chimeric mouse via injection of ESCs into the blastocyst stage of embryo. Pluripotent ESCs able to produce both somatic and germ line cells in Chimeric mice. (Bradley et al., 1984)

2. Adult stem cells

Adult stem cells (ASCs), also known as somatic stem cells, are undifferentiated cells which could found all over the body part after development. ASCs are known as cell source to substitute dying cells and regenerate damaged tissue.

Main cellular characteristics of ASCs are self-renewal capacity and differentiation capacity. ASCs able to differentiate into multiple cell lineages (mesoderm, endoderm and ectoderm). Moreover, ASCs possess great potential to differentiate into many lineages, including, endothelial, skeletal muscle, smooth muscle, cartilage, cardiac tissue, bone. They could proliferate itself and generate into all type of cells and tissues. ASCs also known as their plasticity is donor-dependent, specifically gender, age, and isolated location influence differentiation potential. (Aksu et al., 2008) Unlike embryonic stem cells, ASCs has no ethical issues so it is considered as one of promising cell source for tissue engineering.

Adipose tissue is known as highly complex tissue which consisted with adipocyte, preadipocyte, endothelial cell, and many other types of cells. (Wajchenberg, 2000) Also adipose tissue is a rich source of ASCs which contains pluripotent adipose stromal cells. (Taniguchi et al., 2008, Zuk et al., 2002)

3. Stem cell niche

Stem cell niche is first defined at drosophila ovary stem cell research in cellular and functional level (Xie and Spradling, 2000). Stem cell niche is a specific microenvironment in tissue where stem cells prolonged for undifferentiated state and can differentiate and self-renew in controlled state. Niche controlled balance between maintaining undifferentiated stem cells and differentiating cells in live organism. Stem cell niche refers both *in vivo* and *in vitro* stem cell microenvironment. Within stem cell niche, various niche factors act on stem cells to alter gene expression, and induce to self-renew or differentiate (Birbrair and Frenette, 2016).

Stem cell niche is basically consisting stem cells, niche cells, extracellular matrix (ECM) and other various soluble factors. Stem cells are in close contact with other niche materials and regulated to self-renew of differentiate. ECM plays a pivotal role in cellular processes when they established structural and functional scaffolds in stem cell niche (Hauschka and Konigsberg, 1966). Cells interacts with each ECM molecule with specific receptors called 'integrin heterodimer'. They received signals from each interacting ECM molecules and induce signals into cell for self-renew or differentiation (Leone et al., 2005, Zhu et al., 1999).

3.1 Extracellular matrix in stem cell niche

ECM provides structural and mechanical support and provide chemical and physical characteristics to stem cell niches. It required for cell homeostasis and provide scaffolds to stem cells and store and release soluble factors.(Lane et al., 2014, Brizzi et al., 2012). The ECM is composed with various combination of water, proteins and polysaccharides and each types of niche showed unique features and characteristics by combination of their component (Frantz et al., 2010). The interaction between ECM and stem cells depends on protein composition and their physical properties. Surface topography and stiffness influences contacting stem cell behavior and it means appropriate design of scaffold is needed to culture of stem cells (Lane et al., 2014, Swift et al., 2013, Lu and Atala, 2014). It is certain that stem cell lineage selection in artificial ECM is strictly dependent on ECM protein composition. Soft artificial scaffolds—similar to brain—drive stem cells differentiation into neurogenic lineage (Georges et al., 2006). On the other hand, stiff scaffolds lead stem cell differentiate into myogenic, osteogenic lineages (Engler et al., 2006). Combination of biochemical–mechanical properties of ECM represents to cardiogenic differentiation of stem cells (Engler et al., 2008).

3.2 Cell to ECM communication in stem cell niche: Integrin heterodimer

Integrin is a heterodimeric transmembrane receptors which mediate stem cell bind to ECM and other receptors. Integrin connect extracellular microenvironment to cytoskeleton. Total of 18 α subunits and 8 β subunits gives 24 combination of heterodimers (Prowse et al., 2011). Stem cells in niche interact with ECM via specific integrin heterodimers which is mainly belonging to integrin subunit β_1 subfamily (Raymond et al., 2009, Ellis and Tanentzapf, 2010). Integrin subunit β_1 is generally reported to used in stem cell identification and purification, also maintaining stem cell niche, preserving stem cell population by controlling balance between self-renewal and differentiation (Levesque et al., 2001, Campos, 2005, Veevers-Lowe et al., 2011, Shen et al., 2008). In any cases of integrin subunit β_1 is malfunctioned, stem cell lineage is surprisingly increased to epithelial lineage, by impaired Hedgehog signaling (Jones et al., 2006). When culturing stem cells in 3D artificial scaffolds, integrin subunit β_1 is a stemness determinant and triggers expression of stemness regulators (Lee et al., 2010).

4. Three dimensional culture system

Three dimensional (3D) culture system is provided by artificial synthetic scaffolds to support and regulate cellular activities. Integrin heterodimer mediates cellular attachment to ECM component and these receptors transmit signals and induce signaling cascades into intracellular cytoskeleton. These signaling cascades from integrin heterodimers triggers cellular activities such as cell proliferation, and differentiation(Giancotti and Ruoslahti, 1999).

ECM in 3D culture system able to surround cells in all three dimensions unlike on a petri dishes. These condition allows cells to grow in all direction like *in vivo* condition. These biomimetic condition helps cells to behave similar way in living organism. Within 3D conditions, gene expression of stem cells differ from harvested cell from conventional 2D cultured cells Futhermore, 3D cultured cells showed more accurate depiction when cell polarized, in 2D cultured cells cell only partially polarized (Pampaloni et al., 2007). For Mesenchymal stem cells, different integrin expression occurs when cell were grown in 3D condition and cellular lineage also changed compared to conventional grown cells in 2D conditions(Wozniak et al., 2004, Potapova et al., 2008, Martino et al., 2009). In addition, 3D cultured cells were different from 2D cultured cells in cell migration (Even-Ram and Yamada, 2005). These various changes between 2D and 3D cultured cells were

considered that 3D cultured cell will more closely resemble cellular activities of *in vivo* condition.

Advantages of 3D culture originated from biomimetic culture conditions. In case of drug screening research, 3D cultured cell is much more useful to test drug influences. Gene expression of 3D cultured cell will show more precise results than 2D cultured cells. Since 3D culture system provides more contact space for cellular adhesion, integrin ligation also increased in 3D culture system and intracellular signaling is altered in 3D conditions(Griffith and Swartz, 2006).

Replication of *in vivo* microenvironment with artificial synthetic scaffolds is difficult and requires lots of considerations. Stiffness, composition of scaffolds and cell migration methods also be considered. Poly ethylene glycol (PEG) is a one of synthetic scaffold materials and easily controlled and synthesized. PEG is a hydorophilic polymer which could cross-linked into hydrogel network. PEG could contain high water content and since 1970s, PEG has been used for clinical uses (Davis, 2002). Due to their high water contents, PEG hydrogel could construct soft tissue like scaffolds, which is highly suitable for tissue and cell engineering(Bryant et al., 2004). Also, PEG hydrogel is a biodegradable hydrogel so it is desirable for a various clinical applications

Unfortunately, each cell types doesn't needs same condition of ECM thus, for every types of purposed cells need customized

synthetic scaffolds for stable 3D scaffolds. Even if quality of 3D cultured cells is better than 2d cultured cells, replacement of 2D culture system to 3D culture system may take amount of time and effort.

CHAPTER 3

: Developmental competence of embryo from superovulated mice of different ages by injection of different type of human chorionic gonadotrophin

1. Introduction

Mouse superovulation was one of general protocols for assisted reproductive technology (ART) and standard method has been established (Legge and Sellens, 1994, Johnson et al., 1996). Different strains of mice have been employed for superovulation treatment to date, and strong effect of gonadotrophins drives the negligence of age, strain and drug factors for the treatment. Numerous reports pointed out endogenous factors on the effectiveness of hyperstimulation treatment that yielded superovulation, while different gonadotrophin may yielded different results. (Zarrow and Wilson, 1961, Gates and Bozarth, 1978, Suzuki *et al.*, 1996, Auerbach *et al.*, 2003, Byers *et al.*, 2006)

In this study, I compared the influence of both age and gonadotrophin on the developmental capacity of oocytes retrieved. I used adult (6 to 8 weeks old) or aged (more than 45 weeks old) outbred mice for superovulation and two different human chorionic gonadotrophins (hCGs) were employed (hCG A treated group (Folligon™) and hCG B treated group (Ovidrel™)). As the parameters for monitoring developmental competence of oocytes retrieved, in vitro-culture for both maturation and development, and parthenogenetic activation were employed.

In this chapter, ICR mice was employed as experimental

animals to develop general methods to acquire quality oocytes from mice and to expand cellular resources of embryonic stem cell precursor cells by acquiring oocytes from aged mice.

2. Materials and Methods

Experimental Design

A randomized, prospective model using ICR mouse of different ages (6 to 8 weeks or over 45 weeks old) was employed as experimental animals. Superovulation treatment was proceeded with two different types of human chorionic gonadotrophins (hCGs). Oocyte retrieval and developmental competence of oocytes of Naturally ovulated group (control) and hCG A treated group (Folligon™, MSD animal heath, USA) and hCG B treated group (Ovidrel™, EMD Serono, Germany) were monitored after the injection of different gonadotrophins.

Experimental animals

ICR outbred mice were employed as experimental animals. Mature oocytes were harvested from young (6−8 weeks) or aged (over 45 weeks) female mice after experimental treatments. All animals were maintained under conditions of controlled lightening (14 h of light/10 h of darkness), temperature (20−22°C), and humidity (40–60%). All animal management, breeding, and euthanasic procedures were performed according to the standard protocols of Seoul National University. The experimental protocols were approved by the Institutional Animal Care and Use Committee (approval number

SNU-120220-1). Additionally, experimental samples were managed appropriately, and quality control of the laboratory facility and equipment were conducted.

Collection of mature oocytes

Naturally ovulated oocytes were collected by oviduct flushing of ICR female mice in estrus 16 h after they were mated with a vasectomized male mice. Vaginal smears were performed to check the estrous cycle stage of the female donors. The flushing medium was M2 medium (Sigma-Aldrich, St Louis, MO). For ovarian superovulation, 5 IU of pregnant mare's serum gonadotrophin (PMSG, MSD animal heath, USA) was injected intraperitoneally and ovulation was induced by intraperitoneal injection of 5 IU of different hCG (Folligon™, Ovidrel™) 48 hours later. Oocytes were recovered 16 hours post-hCG. After hormonal treatments females were sacrificed by cervical dislocation. Oocyte maturation at the metaphase II stage was verified by extrusion of the first polar body in the perivitelline space. For this analysis, oocytes were released from cumulus cells through incubation in M2 medium supplemented with hyaluronidase (Sigma-Aldrich; 200 IU/ml) for 5 min at 37°C.

Parthenogenetic activation

To activate oocytes parthenogenetically, oocytes released from cumulus cells were cultured in calcium-free potassium simplex optimized medium (KSOM) supplemented with 10 mM $SrCl_2$ and 5 μg/ml cytochalasin B for 4 hours (h). Oocytes that had been activated parthenogenetically *in vitro* were then cultured in 5 μl droplets of modified Chatot, Ziomek, and Bacister (CZB) medium for a further 120 h at 37°C under an atmosphere of 5% CO2 in air. Pronucleus formation, and development to the two-cell, four-cell, eight-cell, and over stages were monitored under an IX70 inverted microscope (Olympus, Tokyo, Japan) at 6, 24, 48, 72 and 120 h after activation or fertilization.

Statistical analysis

All experiments were replicated more than three times, and the data obtained were subjected to statistical analysis. Not all oocytes retrieved from each experiment were provided because the superovulation treatment yielded different number of oocytes retrieved. To compensate this discrepancy, randomly selected oocytes were allotted to several treatment groups. A generalized linear model (PROC-GLM) created using Statistical Analysis System (SAS) software version 9.1 (SAS Institute, Cary, NC) was used to analyze the data. When a significant model effect was

detected, comparisons among groups were subsequently conducted using the least-squares or Duncan methods. A p-value of less than 0.05 indicated a significant difference.

3. Results

Rate of superovulated mouse after hormone treatment

A total 42 mice (23 adult, 19 aged) were treated with hormones and when more than 25 oocyte retrieval was only considered as being superovulated. In overall group including all age of mice, no significant difference was found between hCG A treated group (Folligon™) and hCG B treated group (Ovidrel™)(Figure 1A). None of aged mice were superovuated (figure 1C) when sixty-seven of hCG A treated group (Folligon) and 100% of hCG B treated group (Ovidrel) were superovulated in 6 to 8 weeks old mice (Figure 1B), which yielded significant difference (p<0.0196).

A

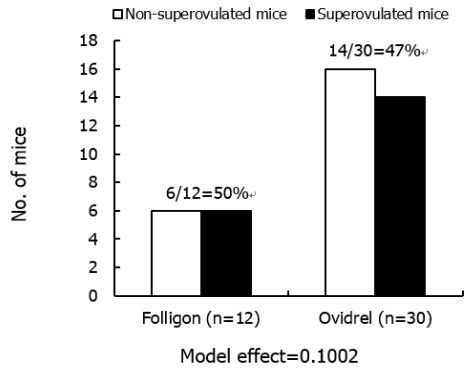

B

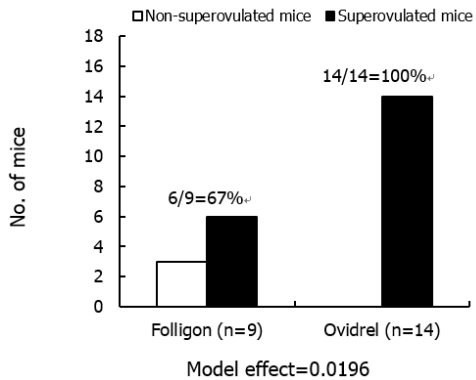

C

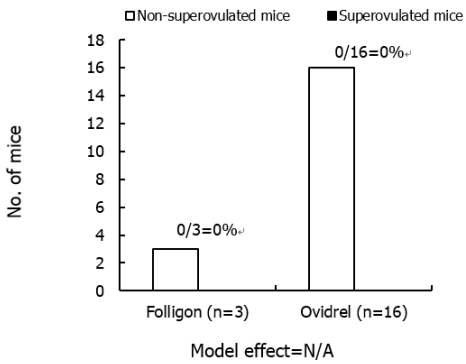

Figure 1. Superovulation of ICR mice with different gonadotrophins. Either 6 to 8 weeks old or 45 to 65 weeks old mice were treated with Folligon™ or Ovidrel™ and the mouse yielding more than 25 ovulated oocytes were considered as a superovulated mouse. Superovulation outcome of (A) total mice (n=42), (B) the mice aged 6 to 8 weeks old (n=23) and (C) the mice aged 45 to 65 weeks old (n=19).

Maturational status of oocytes retrieved from the mice superovulated with different gonadotrophins.

As shown in Table 1, remarkable increase in the number of oocytes retrieved was detected after superovulation treatment within overall aged mice group. Regardless of kinds of gonadotrophins, the total number of retrieved oocytes were increased in hormone treatment group. The proportion of mature oocytes (MII oocytes) retrieved showed no significant difference (44 to 63%) when there were difference in the number of maturing or degenerated oocytes among the treatment groups, while no remarkable tendency was detected.

Table 1. Maturational status of oocytes retrieved from the mice superovulated with different gonadotrophins.

Hormones	Superovulation outcome	No. of mice	Total no. of oocytes retrieved	Mean (±SE) no. of oocytes retrieved	No.(%)[a] of oocytes developed to		No. of oocytes degenerated[c]
					GVBD−MI	MII	
None	Natural cycle	3	15	5.0±0.7[b]	0 (0)[b]	7 (47)	8 (53)[b]
Folligon™	Unsuccessful	6	86	14.3±1.3[bc]	1 (1)[b]	54 (63)	28 (33)[bc]
Ovidrel™	Unsuccessful	16	220	13.8±1.8[c]	77 (35)[c]	96 (44)	47 (21)[c]
Folligon™	Successful	6	190	31.7±2.9[d]	36 (19)[bc]	91 (48)	63 (33)[bc]
Ovidrel™	Successful	14	516	36.9±2.2[d]	114 (22)[c]	303 (59)	94 (18)[c]

GVBD=Germinal vesicle breakdown; MI=Metaphase I; MII=Metaphase II

Model effects on the mean number of oocytes retrieved, the number of oocytes developed to the stage of GVBD−MI and MII, and the number of oocytes degenerated, which were indicated as p value, were less than 0.0001, 0.0173, 0.4262 and 0.028, respectively.

[bcd]Different superscripts within the same parameter indicate significant differences among the treatment, $P<0.05$.

Developmental status of oocytes retrieved from the mice superovulated with different gonadotrophins.

As shown in Table 2, significant difference in the capacity of oocyte activation was detected ($p<0.0096$). All parameters showed remarkable increase in the activation in the fertile than in aged group; 96 to 98% vs. 49 to 57% in pronuclear formation ($P=0.0096$), 94 to 98% vs. 29 to 52% in the first cleavage ($P<0.0001$), 85 to 92% vs. 0 to 41% in 8-cell development ($P<0.0001$), 85 to 89% vs. 0 to 30% in morula compaction ($P<0.0001$) and 72 to 81% vs. 0 to 10% in blastcyst formation ($P<0.0001$). Within the same age, however, no drug effect was detected.

Table 2. Activation of mature oocytes retrieved from 6 to 8 weeks old or 45 to 65 weeks old mice ovulated naturally or superovulated with different gonadrophins.

Ages (wks)	Hormones	No. of mature oocytes cultured	No. (%)[a] of oocytes formed PN	No. (%)[a] of oocytes developed to			
				2-cell	8-cell	Morula	BLST
6-8	None	31	30 (97)[b]	29 (94)[b]	27 (87)[b]	27 (87)[b]	23 (74)[b]
	Folligon™	61	60 (98)[b]	60 (98)[b]	56 (92)[b]	54 (89)[b]	44 (72)[b]
	Ovidrel™	89	85 (96)[b]	85 (96)[b]	76 (85)[b]	76 (85)[b]	72 (81)[b]
45-65	None	7	3 (49)[c]	2 (29)[c]	0 (0)[c]	0 (0)[c]	0 (0)[c]
	Folligon™	21	11 (52)[c]	11 (52)[c]	5 (24)[c]	2 (10)[c]	2 (10)[c]
	Ovidrel™	96	55 (57)[c]	45 (47)[c]	39 (41)[c]	29 (30)[c]	9 (9)[c]

wks=weeks old; PN=pronuclei; BLST=blastocyst

Model effects of treatment on the number of oocytes formed pronulcei, and the number of oocytes developed to the 2-cell, 8-cell, morula and blastocyst stages, which were indicated as p value, were 0.0096, 0.0001, 0.0001, 0.0001, and 0.0001, respectively.

[a]Percentage of the number of MII oocytes retrieved.

[bc]Different superscripts within the same parameter indicate significant differences among the ages, $p<0.05$.

Developmental status of oocytes retrieved from the aged mice superovulated with different gonadotrophins.

As shown in table 3, the number of oocytes formed pronuclei after parthenogenetic activation (43% vs. 52% vs. 61%; p=0.5777) and developed beyond the 2-cell stage embryos (29% vs. 52% vs. 51%; p=0.5079) were not significant different among treatments. While, the number of embryos developed beyond the 8-cell stage were significantly increased in the hCG B (Ovidrel™, p=0.0180), but not the hCG A competed with the control groups (Folligon™, p=0.1667). No difference between two hCGs in the 8-cell stage (24% vs. 46%; p=0.0680).

Table 3. Activation of mature oocytes retrieved after different human chorionic gonadotrophin (hCG) injections into aged (over 45 weeks old) mice.

Hormones	No. of mature oocytes cultured	No. (%)[a] of oocytes formed pronuclei	No. (%)[a] of oocyte developed	
			To 2-cell embryo	Beyond 8-cell embryo
None	7	3 (43)	2 (29)	0 (0)[b]
Folligon™	21	11 (52)	11 (52)	5 (24)[bc]
Ovidrel™	76	46 (61)	39 (51)	35 (46)[c]

Model effects of treatment on the number of oocytes formed pronulcei, and the number of oocytes developed to the 2-cell, and beyond 8-cell stage, which were indicated as p value, were 0.5777, 0.5079, and 0.0164, respectively.

[a]Percentage of the number of MII oocytes retrieved.

[bc]Different superscripts within the same parameter indicate significant differences among the treatment, $p<0.05$

Discussion

Clear evidence was shown in this study showing that kind of gonadotrophin and state of hCG recipients greatly influenced hyperstimulation outcome. Care should be taken to select kind and dose of gonadotrophins especially in aged model animal, which appeared as the efficiency of superovulation treatment in young animals. Although aged mice of 45 weeks or more was reduced the capacity to ovulate oocytes, superovulation treatment still retain development competence and some of those have a capacity to overcome developmental arrest.

Superovulation influences embryonic development *in vitro* or *in vivo* (Ertzeid and Storeng, 2001a, Van der Auwera and D'Hooghe, 2001), oocyte quality , ovarian follicle number (Choi et al., 2011), oocyte degeneration (Tarin et al., 2001), chromosome abnormality (te Velde and Pearson, 2002) and cellular or molecular processes (Miao et al., 2009).

CHAPTER 4

: Screening of integrin heterodimers functionally expressed on the surface of undifferentiated embryonic stem cells in mice

1. Introduction

In a previous report (Lee et al., 2012), a three-dimensional (3D) polyethylene glycol (PEG)-based non-cellular niche promoting embryonic stem cell (ESC) self-renewal was precisely defined by engineering integrin signaling in inbred 129/Ola (E14) ESCs. However, adjustment of ESCs derived from hybrid strain mice to the engineered niche revealed a lack of sustainable self-renewal (Lee et al., 2016), and the mechanical properties of the 3D PEG-based niche showed that effective maintenance of self-renewal was dependent on the genetic background of the ESCs (Lee et al., 2016). These facts emphasize the necessity of developing niches customized to each ESC line from different genetic backgrounds.

There are currently no reports on the development of a 3D PEG-based niche customized to the maintenance of self-renewal of diverse types of ESC. Recently, customization of mechanical properties promoting maintenance of hybrid ESC self-renewal was conducted in a PEG-based 3D hydrogel (Lee et al., 2016), but data on the integrin subunits presented on the surface of ESCs in the undifferentiated state were insufficient to precisely reconstruct a bio-mimicking 3D PEG-based non-cellular niche. Therefore, we examined the types of integrin heterodimers on the surface of

inbred R1 and hybrid B6D2F1 mouse ESCs in the undifferentiated state so that could be compared. The types of integrin subunits expressed in undifferentiated mouse ESCs were identified at the transcriptional and translational levels, and the combinations of integrin α and β subunits were determined by functional assays.

2. Materials and methods

Culture of ESCs

ESCs derived from blastocysts of hybrid B6D2F1 (C57BL6 × DBA2) mice (Lee et al., 2008) and R1 cell line (purchased from Nagy lab) were routinely cultured on mouse embryonic fibroblasts (MEFs) mitotically inactivated by 10 μg/mL mitomycin C (Sigma-Aldrich, St. Louis, MO, USA) in standard ESC culture medium consisting of Dulbecco's modified Eagle's medium (DMEM; Welgene, Daegu, Korea) supplemented with 15% (v/v) heat-inactivated fetal bovine serum (FBS; HyClone, Logan, UT, USA), 1% (v/v) nonessential amino acids (NEAA; Gibco Invitrogen, Grand Island, NY, USA), 0.1 mM β-mercaptoethanol (Gibco Invitrogen), 1% (v/v) lyophilized mixture of penicillin and streptomycin (Gibco Invitrogen), and 1,000 units/mL mouse leukemia inhibitory factor (LIF; Chemicon International, Temecula, CA, USA). Subculture was performed at 3-d intervals and the medium was changed daily during culture. The Institutional Animal Care and Use Committee (IACUC) of Seoul National University (IACUC approval No. SNU0050331-02) approved the research proposal and relevant experimental procedures of this study.

Quantitative real-time polymerase chain reaction (PCR)

An RNeasy Mini Kit (Qiagen, Valencia, CA, USA) was used to extract total mRNA from ESCs, following the manufacturer's instructions, and cDNA synthesis from the extracted mRNA was conducted using a Superscript III first-strand synthesis system (Invitrogen, Carlsbad, CA, USA). Quantification of gene expression was performed using iQ SYBR Green Supermix (Bio-Rad Laboratories, Hercules, CA, USA) in a Bio-Rad iCycler iQ system (Bio-Rad Laboratories). Data on melting curves were collected to check PCR specificity and the β-actin gene was used as an internal control to normalize specific gene expression. mRNA levels were calculated as $2^{-\Delta Ct}$, where Ct = threshold cycle for target amplification and $\Delta Ct = Ct_{\text{target gene}}$ (specific genes for each sample) $- Ct_{\text{internal reference}}$ (β-*actin* for each sample). Table 4 provides general information and sequences for all specific primers designed with mouse cDNA sequences obtained from GenBank using Primer3 software (Whitehead Institute/MIT Center for Genome Research).

Flow cytometry

The harvested ESCs were washed with ice cold Dulbecco's phosphate buffered saline (DPBS; Gibco Invitrogen). Then the ESCs were stained for 30 min at 4° C with PE-conjugated anti-mouse integrin α_5, α_6, α_9, and α_V, FITC-conjugated anti-mouse integrin β_1, β_4, β_5, and β_5, and fluorescence-unconjugated anti-mouse integrin α_8 antibodies. The fluorescence-unconjugated primary antibody was detected by incubation with Alexa Fluor 488-conjugated anti-rabbit IgG. All antibodies were diluted in DPBS supplemented with 2% (v/v) heat-inactivated FBS. Supplementary Table 3 provides detailed information and dilution rates of primary and secondary antibodies. The stained cells were washed and sorted using flow cytometry with a CyAn ADP Analyzer (Beckman Coulter, Inc., Fullerton, CA, USA). The FLOWJO Ver. 7.2.5 software program (Tree Star, Inc., Ashland, OR, USA) was used to analyze acquired data.

Attachment assay

Using a previously described method (Lee et al., 2010), we attached ESCs to extracellular matrix (ECM) ligands. Briefly, 96-

well tissue culture plates were coated with the following concentrations of purified ECM ligands: 0, 40, 100, and 200 μg/mL of fibronectin (Chemicon International); 0, 100, and 200 μg/mL of laminin (Sigma-Aldrich); and 0, 5, and 50 μg/mL of vitronectin (R&D systems, McKinley Place, MN, USA) overnight at 4° C. Blocking of each well was performed by incubation with 10 mg/mL BSA (Sigma-Aldrich) at 4° C for 1 h and 1 × 10^5 ESCs resuspended in standard ESC culture medium were plated into each blocked well. After incubation at 37° C for 2 h, the wells were washed with DPBS to remove non-adherent ESCs from the blocked wells. Adherent ESCs were fixed in 4% (v/v) paraformaldehyde (Sigma-Aldrich) at room temperature for 10 min, stained with 0.1% (w/v) crystal violet (Sigma-Aldrich) in 20% (v/v) methanol (Sigma-Aldrich) for 5 min, and washed extensively with distilled water. Adherent levels were quantified at 570 nm using a microplate reader (VersaMax; Molecular Devices, Sunnyvale, CA, USA) after adding 50 μL of 0.2% (v/v) triton X-100 (Sigma-Aldrich) diluted with distilled water.

Antibody inhibition assay

The wells of 96-well tissue culture plates coated with 40 μg/mL fibronectin, 200 μg/mL laminin, or 5 μg/mL vitronectin overnight at 4° C were blocked with 10 mg/mL BSA for 1 h at 4° C. To inhibit integrin heterodimer function, 1×10^5 ESCs were incubated for 2 h in standard ESC culture medium containing anti-integrin α_5 (5H10-27 [MFR5]), anti-integrin α_6 (NKI-GoH3), or anti-integrin α_V (RMV-7) blocking antibodies at 37° C. Detailed information and dilution rates of the antibodies used are shown in Table 5. The functionally blocked ESCs were plated in each well of 96-well plates coated with ECM proteins and incubated for 3 h at 37° C. Non-adherent ESCs were removed by washing each well with DPBS, and the adherent ESCs were fixed in 4% (v/v) paraformaldehyde for 10 min at room temperature. The fixed adherent ESCs were stained with 0.1% (w/v) crystal violet in 20% (v/v) methanol for 5 min, and each well was washed twice with distilled water. Measurement of adherent levels was conducted using a microplate reader at 570 nm after adding 50 μL of 0.2% (v/v) Triton X-100 diluted with distilled water.

Statistical analysis

All the numerical data derived from each experiment were analyzed in the Statistical Analysis System (SAS) program. Moreover, when a significant main effect was detected by analysis of variance (ANOVA) in the SAS package, the least-square or DUNCAN methods were used for comparison among treatments. Differences among treatments were considered significant when the p value was less than 0.05.

Table 4. Oligonucleotide primers and PCR cycling conditions of mouse integrin subunits.

Genes	GenBank number	Primer sequence		Size (bp)	Temp
		Sense (5' >3')	Anti-sense (5' >3')		
Actb	X03672	TACCACAGGCATTGTGATGG	TCTTTGATGTCACGCACGATT	200	60
Ita1	NM_001033228	TGGCCAACCCAAAGCAAGAA	AGGGCCCACATGCCAGAAAT	200	60
Ita2	NM_008396	TGTGCACCCCCAGAGCACTT	TGTTCACTTGAAGGCCCGGA	181	60
Ita3	NM_013565	AGCAACCTGCAGATGCGAGC	CTCATGCGCATCTTCCCCAG	158	60
Ita4	NM_010576	AGCAAAAAGGCATAGCGGGG	AACGCTGGCTTCCTTCCCAC	160	60
Ita5	NM_010577	AGGCTGCGCTGTGAGTTTGG	TGCCGAGGCAGGATCTGGTA	178	60
Ita6	X63251	AGGTTCGAGTGACGGTGTTT	GTATCGGGGAATGCTGTCAT	185	60
Ita7	NM_008398	GCTTCCCAGACATTGCCGTG	TCCATCCACATCCAGGCCAC	182	60
Ita8	NM_001001309	GCATTCTTGACGTGGGCTGG	ATCCTCTGGGGAGGCAGCAG	154	60
Ita9	NM_133721	GGGGCAGGTCACCGTCTACC	AGCCACATCTGGGAACCCGT	156	60
Ita10	BC115770	GCTGTCTCCATGCCACAGGC	GTGGGGAGGCATCACATCCA	186	60
Ita11	NM_176922	TCCGGTAACCCAGGGCAACT	GCTTCCACACTCGTGCGACC	172	60
Itav	NM_008402	AAGGCGCAGAATCAAGGGGA	CCAGCCTTCATCGGGTTTCC	194	60
Ital	NM_008400	GGAAGCCTGGTGGGCTCAGT	AGCTCAGCACAACCACCCGA	180	60
Itam	NM_008401	CTTTGCAATTGAGGGCACGC	GAAGGCTCCACCTGCCCAGT	150	60
Itad	NM_001029872	TGTGGAGAAGCCCGTCGTGT	AGTGGCAGGCGCACAGTCAT	157	60
Itax	NM_021334	GCTAGGGGACGTGAATGGGG	GGAGGGGATCTGGGATGCTG	165	60
Itae	NM_008399	ACACAAGCCAAAGCCCTTCT	CAGGCTCTTGACTCTGGGTG	186	60
Itb1	NM_010578	CTGGTCCCGACATCATCCCA	CCGTGTCCCACTTGGCATTC	167	60
Itb2	NM_008404	GGTGGCTCAGATCGGGGTTC	TGCACCTGTTGCATTGGCAG	165	60
Itb3	NM_016780	CCCCACCACAGGCAATCAAA	CCCTCTGGGGCATCTCGATT	166	60
Itb4	BC080751	GGCCAGTGGCTCTCTCAGCA	GTGGTCAGCAAGCTCGTGGG	151	60
Itb5	NM_010580	AGGGCGTCCTATGCTCAGGC	AGACACAACGGCCTCGGTCA	161	60
Itb6	NM_021359	GTCCAAGGTGGCTGTGCCTG	TGCGGGAGACAGGGTTTTCA	199	60
Itb7	NM_013566	AAGGAGGGCTCTGCAGTGGG	TACAGTTGGCTGCCAGGGGA	182	60
Itb8	BC125343	GCCTCAAGGTGCGCTCTCAA	AGGCTGCCCCAAGAACCAAG	181	60

Ita=integrin α, Itb=integrin β

Table 5. Primary and Secondary Antibodies of mouse surface integrin.

Antibody Name	Epitope	Catalog Number	Company	Application	Dilution Rate
PE-conjugated armenian hamster anti-mouse/rat integrin α_5	HMa5-1	12-0493	eBioscience	FACS[a]	1:100
PE-conjugated rat anti-human/mouse integrin α_6	GoH3	12-0495	eBioscience	FACS[a]	1:100
PE-conjugated sheep anti-mouse integrin α_9	NS0	FAB3827P	R&D systems	FACS[a]	1:100
PE-conjugated rat anti-mouse integrin α_V	RMV-7	12-0512	eBioscience	FACS[a]	1:100
Alexa Fluor 488-conjugated chicken anti-rabbit IgG (H+L)		A-21441	Molecular Probes	FACS[a]	1:100
FITC-conjugated rat anti-mouse integrin β_1	265917	FAB2405F	R&D systems	FACS[a]	1:100
FITC-conjugated rat anti-mouse integrin β_4	308601	FAB4054F	R&D systems	FACS[a]	1:100
FITC-conjugated mouse anti-mouse integrin β_5	KN52	11-0497	eBioscience	FACS[a]	1:100
FITC-conjugated rat anti-human/mouse integrin β_7	FIB504	11-5867	eBioscience	FACS[a]	1:100
LEAF™ purified rat anti-mouse integrin α_5	5H10-27 (MFR5)	103808	BioLegend®	AIA[b]	1:20
Rat anti-mouse integrin α_6	NKI-GoH3	MAB1378	Millipore	AIA[b]	1:20
LEAF™ purified rat anti-mouse integrin α_V	RMV-7	104108	BioLegend®	AIA[b]	1:20

[a]FACS=Fluorescence-activated Cell Sorting, [b]AIA=Antibody Inhibition Assay

3. Results

Identification of transcriptional expression of integrin subunits on the cell membrane of inbred R1 and hybrid F1 mouse ESCs in undifferentiated state

To determine the types of integrin heterodimers expressed on the membrane of inbred R1 and hybrid F1 mouse ESCs in the undifferentiated state. I monitored the expression of the individual integrin α and β subunits that make up the integrin heterodimers at the transcriptional and translational levels. In the transcriptional analysis of genes encoding 17 integrin α subunits and 8 integrin β subunits, significantly higher levels of expression were observed for integrin α_5 and α_6 (Figure 2a and 2c) and integrin β_1 (Figure 2b and 2d) subunit genes. Minimal levels of expression were detected for integrin α_1, α_3, α_7, α_8, α_9, α_{10}, α_V, α_L, and α_M (Figure 2a and 2c) and integrin β_4, β_5, and β_7 (Figure 2b and 2d) subunit genes. I did not detect any transcriptional expression of integrin α_2, α_4, α_{11}, α_D, α_X, and α_E (Figure 2a and 2c) and integrin β_2, β_3, β_6, and β_8 (Figure 2b and 2d) subunit genes in both strains of mouse ESCs.

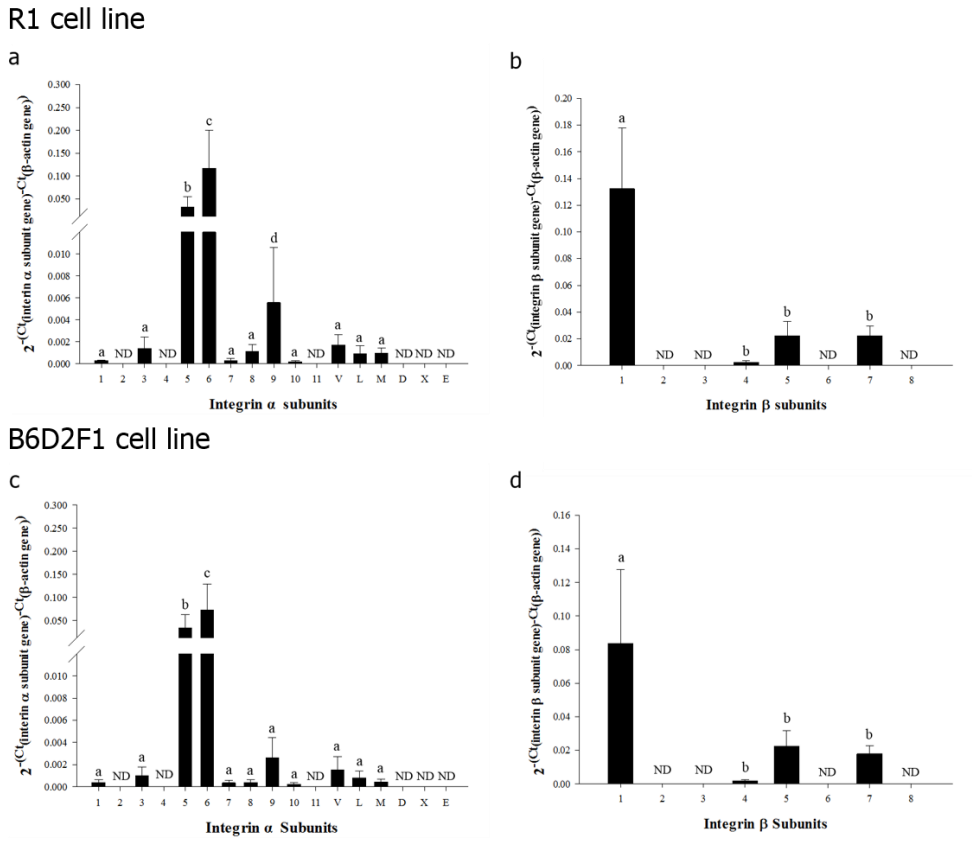

Figure 2. Transcriptional expression of integrin α and β subunit genes in undifferentiated ESCs derived from inbred R1 (129X1/SvJ x 129S1/SvImJ) and hybrid (C57BL6 × DBA2) F1 mice. Messenger RNA levels of integrin α (a and c) and β (b and d) subunit genes in undifferentiated inbred R1 (a and b) and hybrid F1 (c and d) mouse ESCs were examined quantitatively using real-time PCR. All data shown are means ± SD of three independent experiments. $^{a-c}p<0.05$. ND = not detected.

Identification of translational expression of integrin subunits on the membrane of inbred R1 and hybrid F1 mouse ESCs in undifferentiated state

I measured the translational expression of integrin α_5, α_6, α_9, and α_v and integrin β_1, β_4, β_5, and β_7 subunit genes, which showed high levels of transcription (Figure 3). Most of the undifferentiated mouse ESCs expressed integrin α_5, α_6, α_9, and α_v and integrin β_1 subunit proteins on the cellular membrane, and the expression of integrin β_4, β_5, and β_7 subunit proteins were observed in a few undifferentiated inbred R1 and hybrid F1 mouse ESCs. These results indicate that integrin α_5, α_6, α_9, α_v and β_1 subunits are localized on the membrane of inbred R1 and hybrid F1 mouse ESCs in undifferentiated state.

R1 cell line

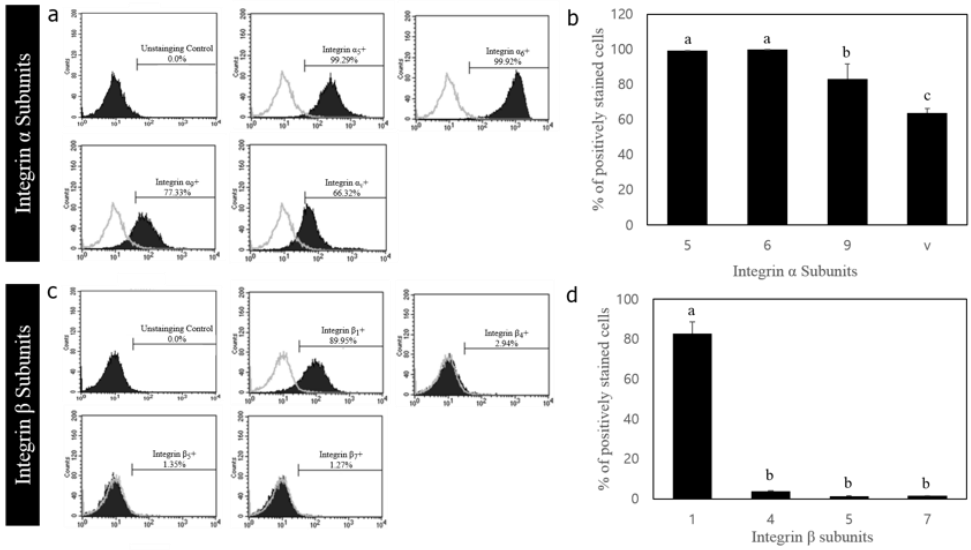

B6D2F1 cell line

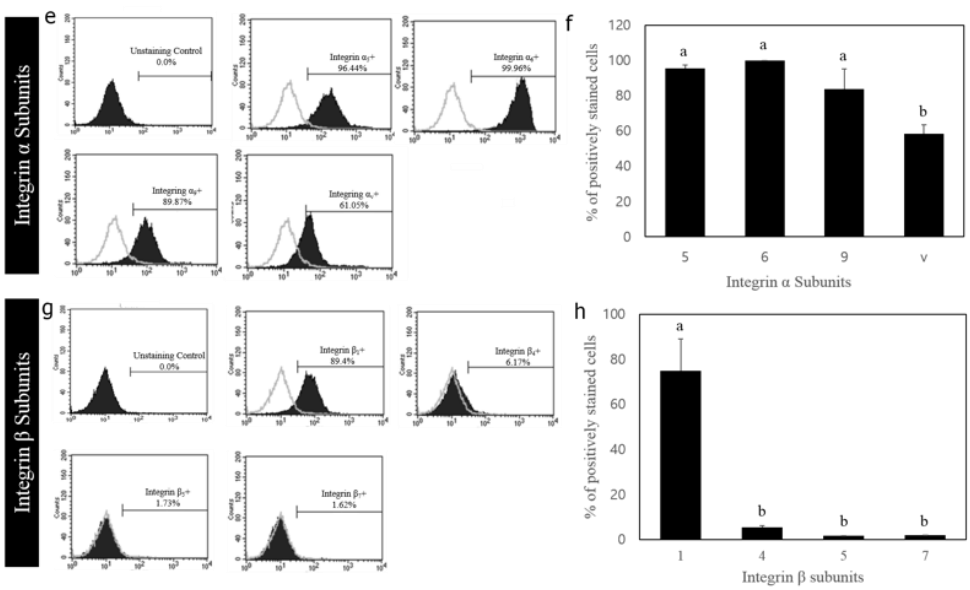

Figure 3. Translational expression of integrin α and β subunit genes in undifferentiated ESCs derived from inbred R1 (129X1/SvJ x 129S1/SvImJ) and hybrid (C57BL6 × DBA2) F1 mice. The translational expression of integrin α (a, b, e and f) and β (c, d, g and h) subunit genes in undifferentiated inbred R1 (a, b, c and d) and hybrid B6D2F1 (e, f, g and h) mice ESCs was measured by flow cytometry. Integrin α_5, α_6, α_9, and α_v subunit proteins were highly expressed at the transcriptional level and were detected on the surfaces of almost all undifferentiated inbred R1 and hybrid B6D2F1 mouse ESCs. Among the four integrin β subunits highly expressed at the transcriptional level, most of the undifferentiated mouse ESCs expressed an integrin β_1 subunit protein on the cell surface, while integrin β_4, β_5, and β_7 subunit proteins were detected on the surfaces of only a few of the undifferentiated mouse ESCs. Figure 3 a, c, e and g are representative FACS analyses of the percentage of cells stained positively with antibodies detecting integrin α or β subunit proteins, and Figure 3 b, d, f, and h are composite averages (means ± SD) of the percentage of cells stained positively with antibodies detecting integrin α or β subunit proteins from three independent experiments. $^{a-c}p < 0.05$.

Determination of integrin heterodimers functionally expressed on the membrane of undifferentiated inbred R1 and hybrid F1 mouse ESCs

Based on transcriptional analysis of each integrin subunit gene, integrin combinations $\alpha_5\beta_1$, $\alpha_6\beta_1$, $\alpha_9\beta_1$ and $\alpha_V\beta_1$ described previously (Prowse et al., 2011), were proposed as candidates for the active integrin heterodimers exhibited in the undifferentiated inbred R1 and hybrid F1 mouse ESCs. I investigated a presence of these integrin heterodimer candidates by estimating the levels of adherent mouse ESCs cultured on natural ECM proteins interacting specifically with each integrin heterodimer and the levels of adherence post-culture of mouse ESCs treated with antibodies specifically blocking each integrin function. Compared to control, both mouse ESCs cultured on fibronectin (Figure 4a, 4d), laminin (Figure 4b, 4e), and vitronectin (Figure 3d, 3f) showed significantly improved adherent levels, indicating that both mouse ESCs could express integrin $\alpha_5\beta_1$, $\alpha_9\beta_1$ and $\alpha_V\beta_1$ which binds specifically with fibronectin, and integrin $\alpha_6\beta_1$, which binds specifically with laminin, and $\alpha_V\beta_1$ which binds specifically with vitronectin on the cell surface in the undifferentiated state.

Specific integrin function-blocked mouse ESCs were incubated with 40 μg/mL fibronectin, 100 μg/mL laminin, or 5 μg/mL vitronectin. Significantly weakened adherent levels were

observed in both strains of mouse ESCs when integrin $\alpha_6\beta_1$ and $\alpha_V\beta_1$ were blocked (Figure 5b, 5c, 5d, and 5f, 5g, 5h), whereas there was no significant decrease in the adherent levels when integrin $\alpha_5\beta_1$ was blocked (Figure 5a and 5e) compared to the control. Based on these results, I confirmed that both strains of mouse ESCs in the undifferentiated state show functional expression of integrin $\alpha_6\beta_1$ and $\alpha_V\beta_1$ on the cellular membrane, while integrin α_5 and α_9 is presented not as a heterodimer, but as a subunit in undifferentiated mouse ESCs.

R1 cell line

a

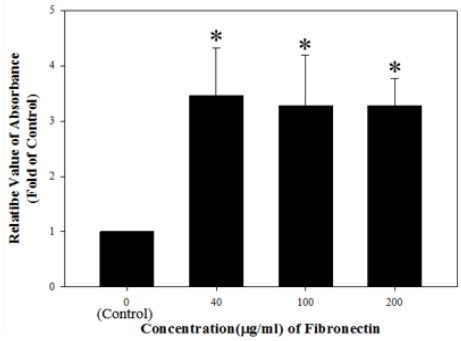

b

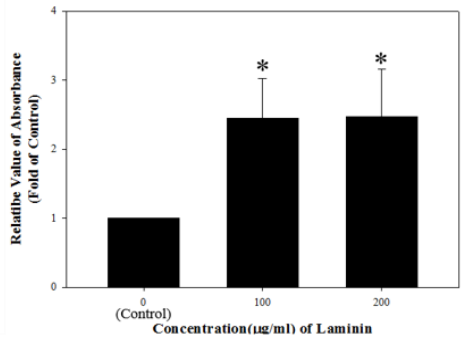

c

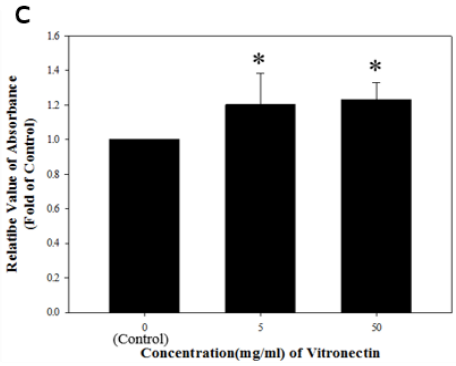

B6D2F1 cell line

d

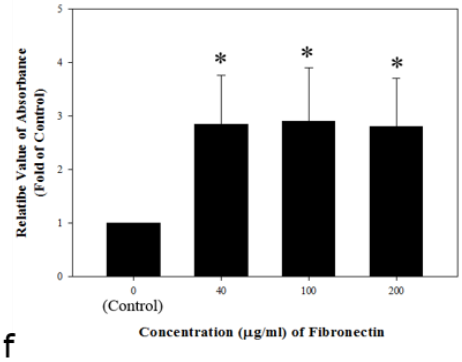

e

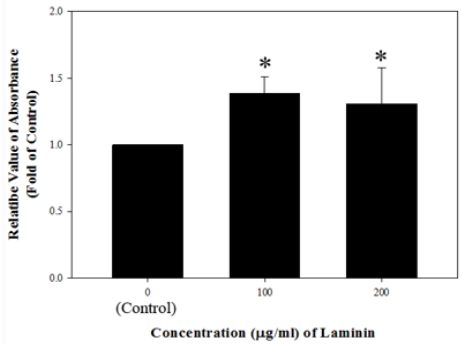

f

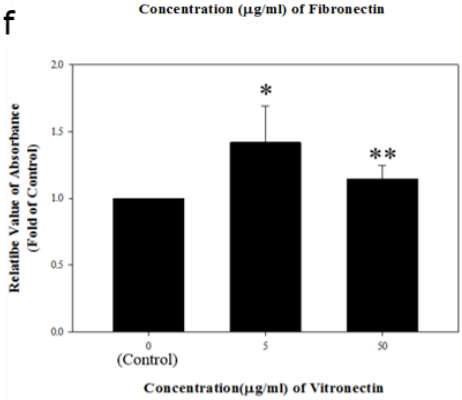

Figure 4. Identification of integrin heterodimers interacting with fibronectin and laminin on the surfaces of undifferentiated ESCs derived from inbred R1 (129X1/SvJ x 129S1/SvImJ) and hybrid (C57BL6 × DBA2) F1 mice. Tissue culture plates (96-well) were coated with 0, 40, 100, or 200 μg/mL fibronectin (a and d) or 0, 100, or 200 μg/mL laminin (b and e) or or with 0, 5, or 50 μg/mL vitronectin (c and f). Uundifferentiated inbred R1 (a, b, and c) and hybrid F1 (d, e, and f) mouse ESCs (1×10^4) were plated in each well. After incubation for 2 h at 37° C, adherent cells were stained with crystal violet and the adhesion level was quantified using a microplate reader. The percentage of maximum adhesion is represented as the optical density of cells plated on ECM protein-free plates. The undifferentiated mouse ESCs cultured on fibronectin-, laminin-, or vitronectin-coated culture plates had significantly higher levels of adhesion than those on ECM protein-free culture plates. All data shown are means ± SD of three independent experiments. $^{*}p<0.05$.

R1 cell line

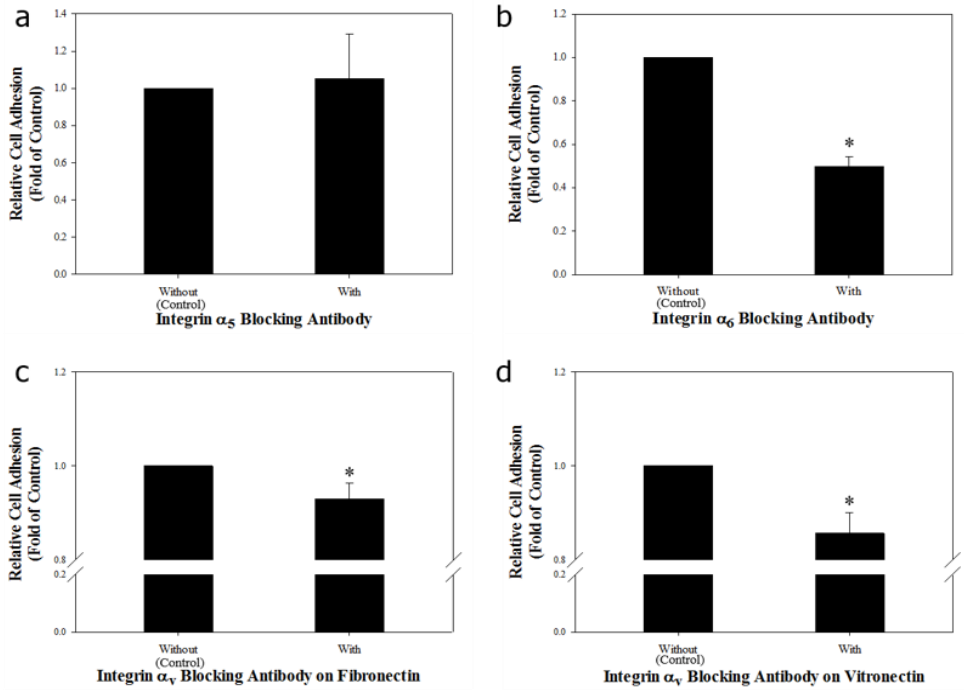

B6D2F1 cell line

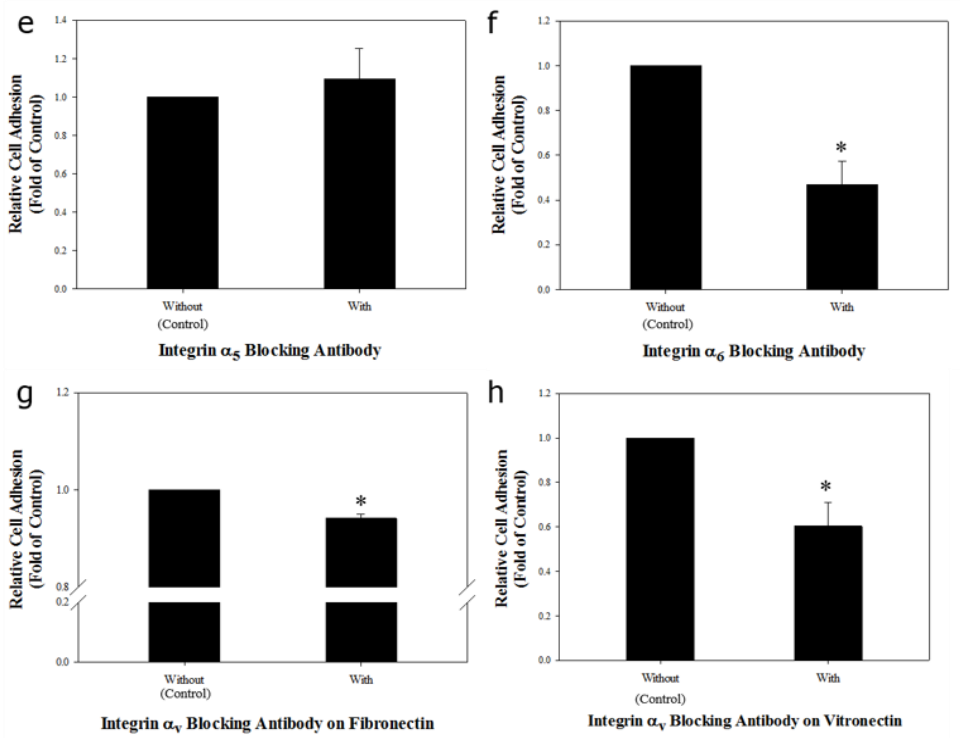

Figure 5. Functional blocking of integrin heterodimers interacting with adhesive proteins in undifferentiated ESCs derived from inbred R1 (129X1/SvJ x 129S1/SvImJ) and hybrid (C57BL6 × DBA2) F1 mice. Undifferentiated inbred R1 (A, B, C and D) and hybrid F1 (E, F, G, and H) mice ESCs were incubated in the absence or presence of anti-integrin α_5 (5H10-27 [MFR5]) (a and e), anti-integrin α_6 (NKI-GoH3) (b and f), or anti-integrin α_V (RMV-7)(c, d, g and h) blocking antibodies and then plated on 40 μg/mL fibronectin-, 100 μg/mL laminin-, or 5 μg/mL vitornectin-coated wells. After incubation for 2 h at 37° C, adherent cells were stained with crystal violet, and quantification of the adhesion level was performed using a microplate reader. As a parameter of functional blocking by antibodies, the relative cell adhesion, which is represented by the optical density of cells plated on each extracellular matrix (ECM) protein-coated well in the absence of any blocking antibodies, was determined. Compared to those without blocking antibodies, undifferentiated hybrid F1 mouse ESCs treated with integrin α_5 blocking antibody showed no significant difference in the rate of attachment to fibronectin (a and e), whereas significantly lower rates of attachment to laminin were observed in the integrin α_6 blocking antibody-treated cells (b and f) and integrin α_V blocking antibody showed a significant decrease in attachment to fibronectin

(c and g) and vitronectin (d and h) compared to those not treated with blocking antibody.. All data shown are means ± SD of three independent experiments. $^{*}p<0.05$.

4. Discussion

Niches that allow for self-renewal or differentiation of stem cells can be precisely designed based on data on integrin family members that mediate intracytoplasmic transduction of extracellular signals derived from ECM proteins. These data are therefore essential to fabricate niches customized to the maintenance of non-differentiation or differentiation induction of inbred R1 and hybrid F1 mouse ESCs. Here, I identified heterodimers or subunits of integrins expressed on the membranes of both strains of mouse ESCs in the undifferentiated state. Through transcriptional analysis of 25 integrin subunits, followed by confirmation of their expression at the translational level, attachment to ECM proteins, and inhibition with blocking antibodies, integrin heterodimers $\alpha_6\beta_1$ and $\alpha_V\beta_1$ and integrin subunits α_5 and α_9 were found to be expressed on the cell membrane. These results suggest that the laminin-interacting integrin $\alpha_6\beta_1$ and vitronectin-interacting integrin $\alpha_V\beta_1$ may play pivotal roles in the maintenance of mouse ESC self-renewal, and that laminin and vitronectin analogs will likely be important in the development of niches customized to the maintenance of hybrid F1 mouse ESC self-renewal. In addition, we propose that integrin

subunits α_5 and α_9 may play important roles in guiding lineage-specific differentiation of both strains of mouse ESCs.

Previously, E14 mouse ESCs derived from blastocysts of an inbred strain showed the presence of integrins $\alpha_5\beta_1$, $\alpha_6\beta_1$, $\alpha_8\beta_1$, $\alpha_9\beta_1$, and $\alpha_V\beta_5$ on the cellular membrane (Lee et al., 2010). However, unlike those, integrins $\alpha_6\beta_1$ and $\alpha_V\beta_1$ were identified in inbred R1 and hybrid F1 mouse ESCs. The difference in the integrin heterodimers presented on the surfaces of ESCs may explain why synthetic niches customized to maintaining self-renewal of E14 mouse ESCs are not effective in maintaining self-renewal of B6D2F1 mouse ESCs (Lee et al., 2016). These results demonstrate that integrin expression patterns are dependent on genetic background despite being from the same species, necessitating synthetic niche customization according to genetic background as well as species.

Integrins $\alpha_6\beta_1$ and $\alpha_V\beta_1$ were observed on the surfaces of undifferentiated mouse ESCs (Figures 4), suggesting that the presence of laminin and vitronectin in the niches around the blastocyst inner cell mass (ICM) may be important to maintain self-renewal in these cells. Unfortunately, there is no direct evidence for the expression of laminin and vitronectin in the blastocyst ICM derived from mice. Several reports demonstrated

that *in vitro* culture of pluripotent stem cells on laminin- (Domogatskaya et al., 2008) or vitronectin- (Kaini et al., 2016) coated culture plates can stimulate the maintenance of self-renewal. In contrast, we propose that integrins $\alpha_6\beta_1$ and $\alpha_V\beta_1$ may play more pivotal roles in initiating early stage differentiation of undifferentiated hybrid B6D2F1 mouse ESCs than in maintaining self-renewal, supported by the fact that there are many problems in differentiation using laminin signaling-free ICM during embryogenesis (Li et al., 2002) and mouse ESCs cultured on laminin or vitronectin easily lose their pluripotency (Heydarkhan-Hagvall et al., 2012, Hayashi et al., 2007). Those contradict statement for laminin and vitronectin in maintaining pluripotency or initiating early differentiation could be occurred by different stage of ESCs/blastocyst or by their diverse genetic background. Further studies on the distribution of ECM proteins in blastocysts and their cell to ECM communications are required to confirm this.

In the microenvironment that generates a fetus from the blastocyst ICM during embryogenesis, inactive integrin subunits can induce cytological, structural, and functional changes in fetal cells following three-germ layer differentiation of the ICM (Vitillo et al., 2016). In this study, integrin subunits α_5 was observed in inactive forms on cell membranes (Figures 3 and 4), indicating that signals

derived from the interaction between fibronectin and integrin heterodimers with integrin subunit α_8 may be important in early embryonic development of the ICM; this is supported by reports that fibronectin induces differentiation of pluripotent stem cells into specific cell lineages (Kang et al., 2015). Therefore, knowledge of the inactive integrin subunits expressed in specific cells is important in the development of synthetic niches customized to guiding a particular cell fate.

In conclusion, transcriptional, translational, and functional screening of integrins demonstrated that integrins $\alpha_6\beta_1$ and $\alpha_V\beta_1$ are expressed on the surface of undifferentiated inbred R1 and hybrid F1 mouse ESCs. Expression of the inactive integrin subunits α_5 and α_9 was also demonstrated. The identified active integrin heterodimers may be useful in maintaining mouse ESCs derived from both strains in the undifferentiated state. Moreover, these results will greatly improve the applicability of synthetic niches with respect to the maintenance of self-renewal in mouse ESCs derived from a variety of genetic backgrounds.

CHAPTER 5

: Difference in suitable mechanical properties of three-dimensional, synthetic scaffolds for self-renewing of mouse embryonic stem cells of different genetic backgrounds

1. Introduction

Biomimetic three-dimensional (3D) hydrogels have been used to manipulate stem cells based on their activities supporting self-renewal. In our previous studies, self-renewal activity of mouse embryonic stem cells (ESCs) was maintained on polyethylene glycol (PEG)-based 3D scaffolds of different compositions, regardless of the presence or absence of a self-renewal promoting factor(Lee et al., 2010, Lee et al., 2012). An inbred 129/Ola (E14) ESC line was employed for 3D culture in previous studies, but we recognized the need to evaluate the versatility of the hydrogel against ESC lines with different genetic backgrounds, as genotypic differences could induce phenotypic changes(Jennings, 1911, Johannsen, 2014, Simpson et al., 1997, Lehner, 2013). A system optimized for a specific genetic background may not work smoothly in cells with other genetic backgrounds (Baharvand and Matthaei, 2004). In this study, I evaluated whether cell genetic background influences the mechanical properties of 3D synthetic scaffolds designed for ESC self-renewal by culturing inbred and F1 hybrid mouse ESC lines in hydrogels with different mechanical properties.

2. Materials and methods

Experimental Design

As a first experiment, two mouse ESC lines, inbred R1 (129X1/SvJ x 129S1/SvImJ) and hybrid B6D2F1 (C57BL6 x DBA2), were embedded into the hydrogel customized for E14 ESC line and the expression of self-renewal-related SSEA-1, Oct4 and Nanog proteins were monitored by flow cytometry. In the second series of experiments, R1 and F1 ESC lines were seeded into the hydrogel with varied types (3, 4, and 8-arm) and concentrations [7.5%, 10.0%, 12.5%, 15.0% (wt/v)] of polyethylene glycol (PEG). The ESCs were cultured in the designed 3D scaffolds for 7 days. ESC proliferation and viability were measured on day 1 or 7 of culture. In the third series of experiments, self-renewal activity after being embedded in the hydrogel of optimal properties for each ESC line was screened, and stemness-related gene (*Oct4*, *Nanog*, *Sox2*, *Tert*, *Klf4*, *Cdh1*) and protein expressions [alkaline phosphatase (AP) activity, Oct4 and Nanog were monitored.

Culture of ESCs

R1 (ATCC) and F1 (B6D2F1) ESCs were routinely cultured on

mouse embryonic fibroblasts (MEFs) treated with 10 μg/ml mitomycin C (Sigma-Aldrich, St. Louis, MO) in standard ESC culture medium consisting of Dulbecco's modified Eagle's medium (DMEM; Welgene, Daegu, Korea) supplemented with 15% (v/v) fetal bovine serum (FBS; HyClone, Logan, UT), 1% (v/v) nonessential amino acids (NEAA; Gibco Invitrogen, Grand Island, NY), 0.1 mM β-mercaptoethanol (Gibco Invitrogen), 1% (v/v) lyophilized mixture of penicillin and streptomycin (Gibco Invitrogen) and 1,000 untis/ml mouse leukemia inhibitory factor (LIF; Chemicon International, Temecula, CA)(Gong et al., 2009, Lee et al., 2008). Subculturing was performed at 3-day intervals and the medium was changed daily during culture. The Institutional Animal Care and Use Committee, Seoul National University, approved research proposal and relevant experimental procedure of this study (approval number: SNU0050331-02).

Formation of PEG-based hydrogel, encapsulation of ESCs into poly(ethylene glycol) (PEG)-based hydrogel and culture

Vinylsulfone (VS; Sigma-Aldrich)-functionalized 3-arm, 4-arm and 8-arm PEG (PEG-VS) were synthesized as previously described[10] and dicystein-containing peptides with an intervening

matrix metalloproteinase (MMP)-specific cleavage site (Ac-GCRD-GPQGIWGQ-DRCG-NH2) were used as crosslinker connecting among PEG-VS(Lutolf et al., 2001). Moreover, according to previously described protocols (Lee et al., 2010), construction of the PEG-based hydrogel, incorporation of cell adhesion peptides to the PEG-based hydrogel and encapsulation of ESCs into the hydrogel were performed. Subsequently, ESCs encapsulated into the hydrogel were cultured in standard ESC culture medium at 37° C in a humidified atmosphere of 5% CO_2 in air and replacement of medium was conducted every day. The cultured ESCs were retrieved from the hydrogel by incubating in 10 mg/ml collagenase I (Sigma-Aldrich) solution for 10 minutes and enumerated using a hemocytometer.

Adhesion peptide synthesis and purification

Synthesis and purification of adhesion peptides were conducted as previously described(Lutolf et al., 2001, Lutolf and Hubbell, 2003). Briefly, an automated peptide synthesizer (PerSpective Biosystems, Farmington, MA) adjusting standard Fmoc/HBTU/HOBT chemistry was used for synthesizing adhesion peptides and C18 chromatography (Biocad 700E; PerSpective Biosystems) was used

for purifying synthesized adhesion peptides. Subsequently, identification of synthetic adhesion peptide sequences of AcGCGWGRGDSPG, GCRDTTSWSQG and AcGCRRRRDRD AEIDGIELG was conducted by matrix-assisted laser desorption ionization/time-of-flight (MALDI-TOF) mass spectrometry.

Flow cytometry

A 4% (v/v) formaldehyde (Sigma-Aldrich) fixative solution was used for fixation of ESCs. After washing in ice cold PBS (Gibco Invitrogen), fixed ESCs in PBS supplemented with 2% (v/v) heat-inactivated FBS were stained for 1 hour at 4° C with unconjugated anti-stage specific embryonic antigen (SSEA-1) primary antibody and the detection of primary antibody was performed by FITC-conjugated secondary antibody. Moreover, for staining Oct4 and Nanog, fixed ESCs were incubated for 1 h at 4° C with Alexa Fluor® 647-conjugated anti-Oct3/4 and Alexa Fluor® 488-conjugated anti-Nanog primary antibodies diluted in Hanks' Balanced Salt Solution (HBSS; Gibco Invitrogen) supplemented with 0.1% (w/v) saponin (AppliChem Gmbh, Darmstadt, Germany) and 0.05% (w/v) sodium azide (Sigma-Aldrich). Supplementary Table 1 shows detailed information and dilution rate of primary or

secondary antibodies used in this study. Subsequently, the stained cells were washed sufficiently and sorted using flow cytometry with a CyAn™ ADP Analyzer (Beckman Coulter, Inc., Fullerton, CA). Moreover, FLOWJO Ver. 7.2.5 software program (Tree Star, Inc., Ashland, OR) was used for analyzing acquired data.

Monitoring of proliferation activity

On 1 day and 7 days of culture, the cell counting kit (CCK)-8 reagent (Dojindo Laboratories, Kumamoto, Japan) was added to each well containing a variety of the hydrogels encapsulating ESCs. After 3 hours of incubation, the absorbance of CCK-8 was measured at 450 nm using Bio-Rad microplate reader Model-550 (Bio-Rad Laboratories, Hercules, CA). Subsequently, proliferation activity of ESCs was calculated as A_{day7}/A_{day1}, where A_{day7} = absorbance on day 7 of culture, and A_{day1} = absorbance on day 1 of culture. Herein, cell viability was represented by absorbance measured by a CCK and direct proportion of absorbance and cell number was described in Supplementary Figure 1.

Real-time PCR

The RNeasy Mini Kit (Qiagen, Valencia, CA) was used for extracting total mRNA and cDNA synthesis from the extracted mRNA was conducted by a Superscript III first-strand synthesis system (Invitrogen^{TM}, Carlsbad, CA) according to each manufacturer's instruction. Subsequently, quantification of gene expression was performed with iQ^{TM} SYBR® Green Supermix (Bio-Rad Laboratories, Hercules, CA) under the Bio-Rad iCycler iQ system (Bio-Rad Laboratories). Data on melting curve were collected to check the PCR specificity and β-actin was used as an internal control for normalization of the specific gene expression. Relative mRNA level was calculated as $2^{-\Delta\Delta Ct}$, where Ct = threshold cycle for target amplication, $\Delta Ct = Ct_{\text{target gene}}$ (specific genes for each sample)$-Ct_{\text{internal reference}}$ (β-actin for each sample), and $\Delta\Delta Ct = \Delta Ct_{\text{sample}}$ (treatment sample in each experiment)$-\Delta Ct_{\text{calibrator}}$ (control sample in each experiment). Table 6 shows general information and sequences of all the specific primers designed with cDNA sequences obtained from GenBank for mouse and by Primer3 software (Whitehead Institute/MIT Center for Genome Research).

Alkaline phosphatase (AP) staining

ESCs fixed in 4% (v/v) formaldehyde for 15 minutes at room temperature were washed twice with PBS. Subsequently, staining of the fixed cells with AP staining solution consisting of 0.1 M Tris buffer (pH 8.2) supplemented with 0.2 mg/ml naphthol AS-MX phosphate (Sigma-Aldrich), 2% (v/v) dimethyl formamide (Sigma-Aldrich), and 1 mg/ml Fast Red TR salt (Sigma-Aldrich) was conducted for 90 minutes at room temperature. Then, after washing twice with PBS, the stained cells were observed under a Nikon Eclipse TE2000-U microscope (Nikon, Tokyo, Japan) equipped with a JENA ProgRes camera (JENOPTIK, Berlin, Germany).

Immunocytochemistry

After washing ESCs fixed in 4% (v/v) formaldehyde for 15 min at room temperature, the fixed ESCs were incubated for 18 hours at 4°C with unconjugated anti-Oct3/4 primary antibody diluted in HBSS supplemented with 0.1% (v/v) Triton X-100 (Sigma-Aldrich) and unconjugated anti-SSEA-1 primary antibody diluted in PBS supplemented with 2% (v/v) heat-inactivated FBS. Subsequently, primary antibodies against Oct3/4 and SSEA-1 were detected by incubating Alexa Fluor® 568- and Alexa Fluor® 488-conjugated secondary antibodies, respectively, for 2 hours at 4° C.

Detailed information and dilution rates of the antibodies used are shown in Table 7. Then, the stained ESCs were rinsed twice with ice cold PBS, counterstained for 15 minutes with Mounting medium for fluorescence with DAPI (Vector Laboratories, Inc., Burlingame, CA), and observed under Nikon Eclipse TE2000-U microscope (Nikon) equipped with a JENA ProgRes camera (JENOPTIK).

Statistical analysis

The Statistical Analysis System (SAS) program was used for analyzing statistically all the numerical data shown in each experiment. In case of data resulted from flow cytometry analysis, each treatment was compared by DUNCAN or the least-square method, when a significance of the main effects was detected through variance (ANOVA) analysis in the SAS package. Whereas, in case of data resulted from proliferation activity and gene expression analysis, a generalized linear model (PROC-GLM) in the SAS package was used to evaluate the effect of each treatment. Significant differences among treatments were determined where the P-value was less than 0.05.

Table 6. Oligonucleotide Stemness genes primers and PCR cycling conditions of mouse stemness-related genes.

Genes	GenBank number	Primer sequence		Size (bp)	Temp
		Sense (5' >3')	Anti-sense (5' >3')		
β-actin	X03672	TACCACAGGCATTGTGATGG	TCTTTGATGTCACGCACGATT	200	60
Oct-4	M34381	GAGGAGTCCCAGGACATGAA	AGATGGTGGTCTGGCTGAAC	135	60
Nanog	AY455282	CACCCACCCATGCTAGTCTT	ACCCTCAAACTCCTGGTCCT	151	60
Sox2	AB108673	CAGCTCGCAGACCTACATGA	TGGAGTGGGAGGAAGAGGTA	152	60
Tert	AF051911	GAAGTTCATCTCGTTGGGGA	CAGTATGTGTCCATCAGCCA	183	60
Klf4	NM_010637	CTGAACAGCAGGGACTGTCA	GTGTGGGTGGCTGTTCTTTT	218	60
Cdh1	NM_009864	CAAGGACAGCCTTCTTTTCG	TGGACTTCAGCGTCACTTTG	165	60

Table 7. Primary and Secondary Antibodies of mouse stemness related marker.

Antibody Name	Catalog Number	Company	Application	Dilution Rate
Mouse anti-SSEA-1 IgM	MAB4301	Chemicon	FACS	1:100
Alexa Fluor® 647 rat anti-mouse Oct3/4	51-5841	eBioscience	FACS	1:100
Alexa Fluor® 488 rat anti-mouse Nanog	53-5761	eBioscience	FACS	1:100
Rabbit anti-Oct-3/4 IgG	sc-9081	Santa Cruz	IF	1 :100
Mouse anti-SSEA-1 IgM	sc-101462	Santa Cruz	IF	1 :100
Alexa Fluor 568® Goat Anti-Rabbit IgG (H+L)	A11036	Molecular Probes	IF	1 :200
Alexa Fluor 488® Goat Anti-Mouse IgM	A21042	Molecular Probes	FACS IF	1 :100 1 :200

FACS=Fluorescence-activated cell sorting, IF=Immunofluorescence.

3. Results

Effects of a 3D hydrogel customized for E14 ESC self-renewal on other ESC lines

Decreased protein expression by R1 and F1 ESCs cultured inside hydrogels was detected after 3D culture optimized for E14 ESCs, compared with control ESCs cultured on feeder-containing 2D scaffolds. Significant differences in Oct4 expression by R1 cells (Figure 6a) and of Nanog by F1 ESCs were detected (Figure 6b). These results suggest that each cell line required a scaffold with different mechanical properties for optimal self-renewal *in vitro*.

R1 cell line

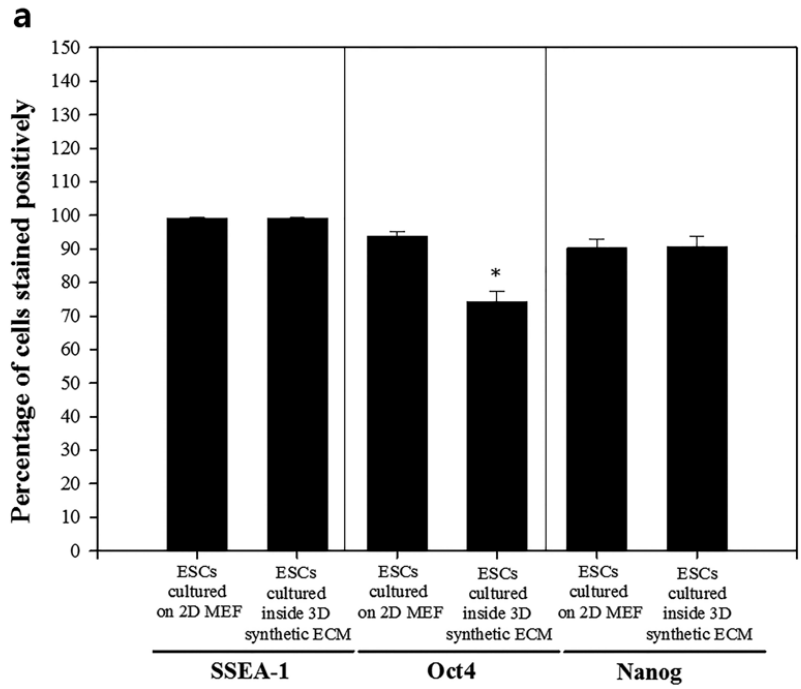

B6D2F1 cell line

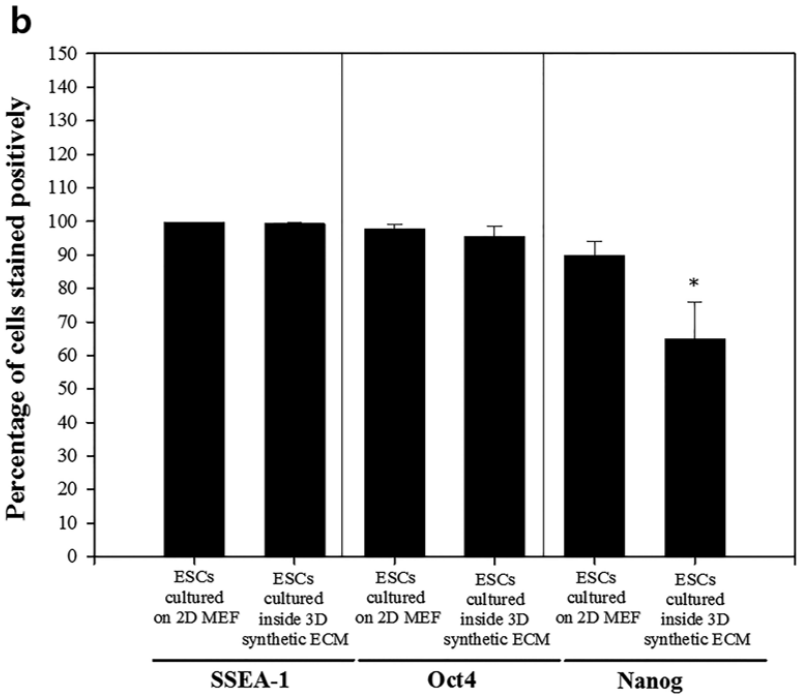

Figure 6. Effects of a three-dimensional (3D) synthetic hydrogel scaffold customized for E14 embryonic stem cells (ESCs) on maintaining ESC pluripotency of other cell line. A hydrogel constructed by 3-arm polyethylene glycol (PEG) was employed as the 3D synthetic hydrogel and inbred R1 (a) and hybrid B6D2F1 (b) ESCs were cultured for 3 weeks inside the hydrogel scaffold (Lee et al. 2010). For estimating ESC pluripotency, the expressions of SSEA-1, Oct4 and Nanog proteins were analysed by flow cytometry. Compared with the ESC lines cultured in conventional, two-dimensional (2D) culture system, decreased expression of Oct4 in R1 and Nanog in F1 ESCs were detected after cultured in the 3D hydrogel scaffold. All data shown are means±SE of three independent replicates. $^{*}p<0.05$ vs. 2D.

Suitable hydrogel scaffold mechanical properties for proliferation of each ESC line

Predominant R1 ESC colony formation activity was detected at 7.5 and 10.0% in the four-arm and at 7.5% in the eight-arm PEG scaffolds compared to activity in the other treatments (Figure 7a). The 7.5, 10.0, 12.5, and 15.0% treatments with the three-arm PEG scaffolds yielded the best properties for the F1 ESC line among the other treatments (Figure 7b). However, colony formation occurred inside the hydrogels under all 3D conditions. The 7.5% with the four-arm PEG scaffolds (10.04 vs. 0.16–4.39; $p = 0.0006$) was the optimal cell proliferation treatment for R1 cells. F1 cells tended to show better proliferation in the 10.0% three-arm PEG scaffolds (4.1 vs. 0.45–2.38; $p = 0.1541$) (Figure 8). We subsequently determined that the mechanical properties of the 7.5% four-arm and 10.0% three-arm PEG-based hydrogels were suitable for the R1 and F1 ESC lines, respectively.

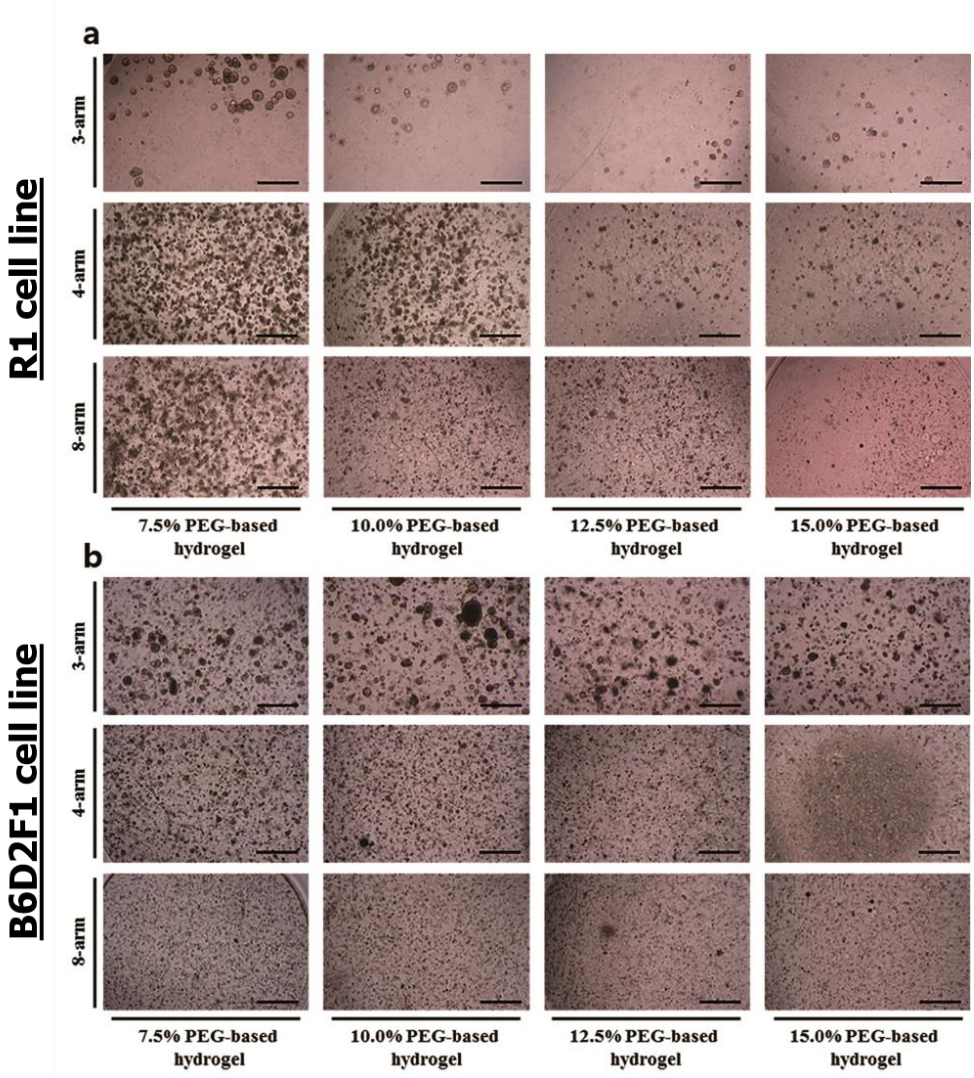
R1 cell line
B6D2F1 cell line
a
b
3-arm
4-arm
8-arm
7.5% PEG-based hydrogel
10.0% PEG-based hydrogel
12.5% PEG-based hydrogel
15.0% PEG-based hydrogel

Figure 7. Colony formation of mouse embryonic stem cells (ESCs) cultured inside three-dimensional (3D) polyelene glycol (PEG)-based hydrogel with different mechanical properties. Hydrogels of different mechanical properties were constructed by the conjugation of 7.5, 10.0, 12.5 or 15.0% (wt/v) 3-, 4- or 8-arm PEG functionalized by vinylsulfone with crosslinkers, and inbred R1 (a) and hybrid B6D2F1 (b) ESCs were employed for the 3D culture. After culturing for 7 days, colony formation inside the hydrogel was observed in all 3D conditions designed under inverted microscope. Among compositions, R1 ESCs derived colonies predominantly in 7.5 and 10.0% 4-arm and 7.5% 8-arm PEG-based hydrogel, whereas predominant formation was detected at 7.5 to 15.0% 3-arm PEG-based hydrogel. Three replicates. Scale bar, 600 μm.

R1 cell line

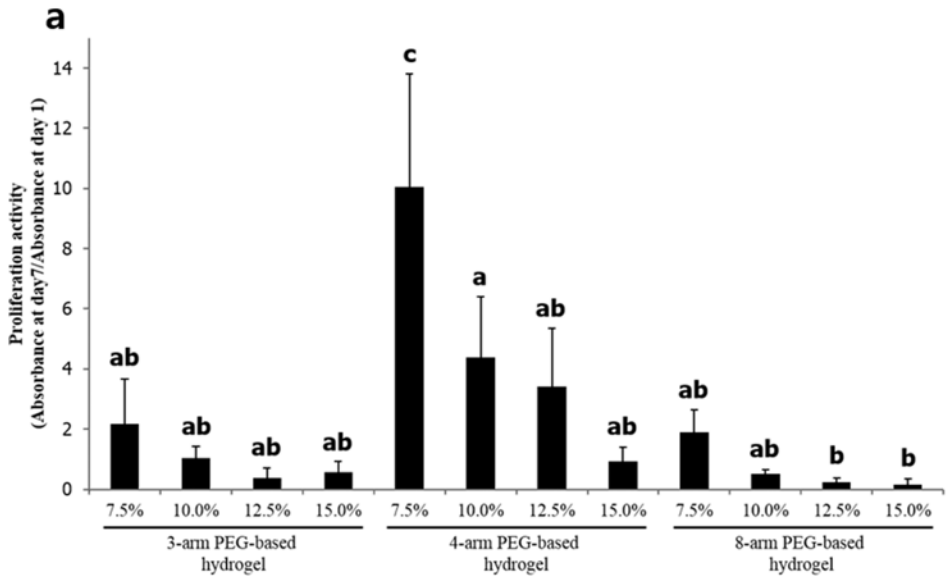

B6D2F1 cell line

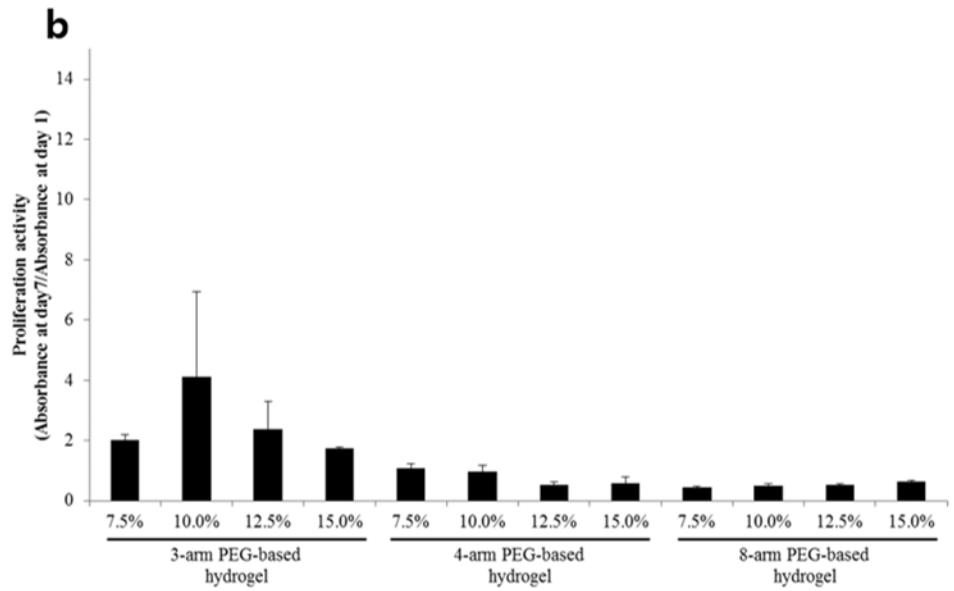

Figure 8. Proliferation activity of inbred R1 (a) and hybrid B6D2F1 (b) embryonic stem cells (ESCs) cultured inside three-dimensional (3D) polyethylene glycol (PEG)-based hydrogel scaffolds of different mechanical properties. The hydrogel of different properties was conducted by the conjugation of vinylsulfone-functionalized, 7.5, 10.0, 12.5 or 15.0% (wt/v) PEG with 3-, 4- or 8-arm with crosslinkers and ESCs were cultured in each hydrogel for 7 days. Viability was measured on day 1 and 7 of culture with ELISA using a cell counting kit (CCK) and proliferation activity was calculated by dividing CCK absorbance on day 7 of culture with the absorbance on day 1 of culture. Among compositions, R1 ESCs cultured inside 7.5% 4-arm PEG-based hydrogel showed significantly the highest proliferation activity. While significant difference was not detected, the highest proliferation was detected at 10.0% 3-arm PEG-based hydrogel in F1 ESCs (B). All data shown are means±SE of five independent replicates. Model effects shown as p value were 0.0006 (a) and 0.1541 (b). $^{abc}p<0.05$.

Effects of the 3D synthetic scaffolds customized to each ESC line in proliferation on maintenance of ESC self-renewal

The gene expression patterns differed between the two cell lines, but all genes were expressed in 3D culture (Figure 9). All genes were transcribed without a decrease in expression, and *Oct4*, *Nanog*, *Sox2,* and *Tert* expression were significantly ($p < 0.05$) upregulated in R1 ESCs. In contrast, *Oct4*, *Nanog*, and *Sox2* expression decreased significantly ($p < 0.05$) after 3D culture of the F1 ESC line. The expression patterns were more prominent in the 3D than in the 2D feeder-containing cultures. All genes in R1 ESCs were upregulated after 3D culture, whereas most genes were downregulated in F1 ESCs, except *Klf*4. However, alkaline phosphatase activity and Oct4 and SSEA-1 were still detected and expressed translationally in both ESC lines cultured in hydrogel scaffolds (Figure 10).

R1 cell line

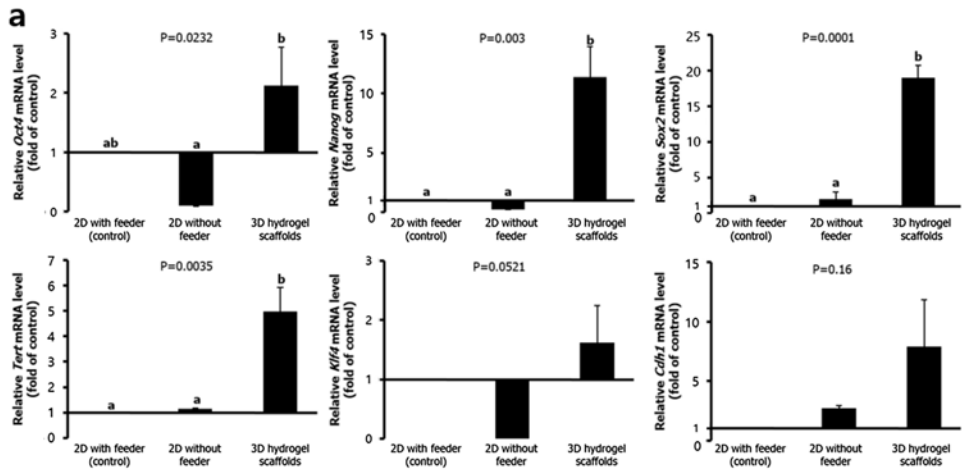

B6D2F1 cell line

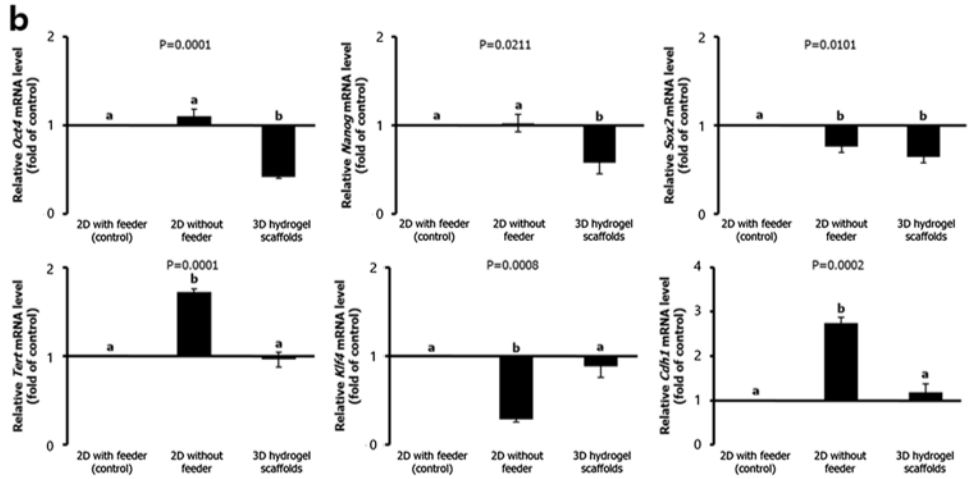

Figure 9. Transcriptional regulation of self-renewal-related genes in inbred R1 (a) and hybrid B6D2F1 (b) embryonic stem cells (ESCs) cultured in two-dimensional (2D) with or without mouse embryonic fibroblasts (MEFs) and inside three-dimensional (3D) polyethylene glycol (PEG)-based hydrogel of optimal properties in this study. R1 and F1 ESCs were cultured inside the hydrogel of 7.5% (wt/v) PEG with 4-arm and 10.0% PEG with 3-arm, respectively. On day 7 of culture, the expression of self-renewal-related genes was analyzed by real-time PCR. In R1 ESCs, no decreased expression of the genes was detected, while relative decrease in *Oct4*, *Nanog* and *Sox2* expressions was detected in F1 ESCs. The difference of expressional patterns between feeder-free 2D and 3D was different between two lines. All data shown are means±SE of three independent replicates. $^{ab}p<0.05$.

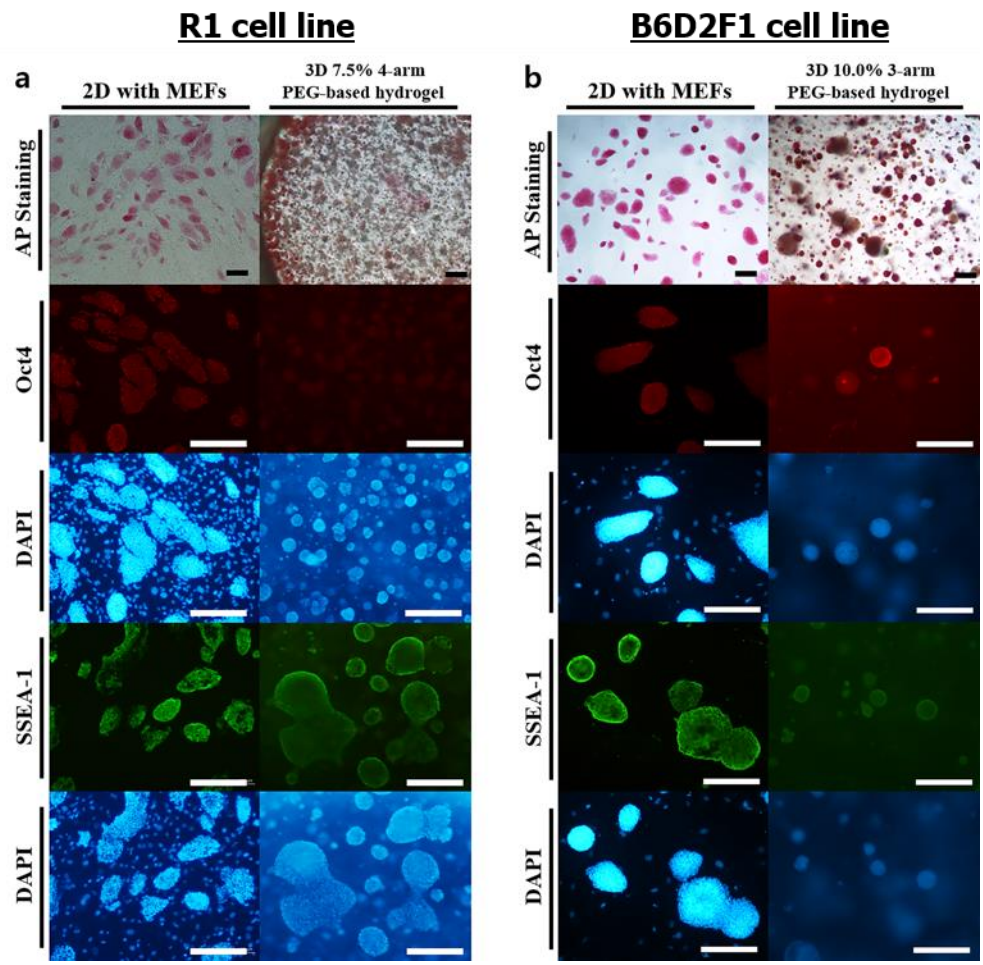
R1 cell line
B6D2F1 cell line
a
b
2D with MEFs
3D 7.5% 4-arm PEG-based hydrogel
3D 10.0% 3-arm PEG-based hydrogel
AP Staining
Oct4
DAPI
SSEA-1
DAPI

Figure 10. Analysis of self-renewal-related, alkaline phosphatase (AP), Oct4 and SSEA-1 protein expression in inbred R1 (a) and hybrid B6D2F1 (b) embryonic stem cells (ESCs). ESCs were cultured in two-dimensional (2D) with mouse embryonic fibroblasts (MEFs) and inside three-dimensional (3D) polyethylene glycol (PEG)-based hydrogel of optimal properties in this study. R1 and F1 ESCs were cultured inside the hydrogel of 7.5% (wt/v) PEG with 4-arm and 10.0% PEG with 3-arm, respectively. On day 7 of culture, protein activity was monitored under a confocal microscopy and all ESC lines were positive for each protein. Scale bar, 300 μm.

4. Discussion

I reconfirmed that the synthetic, 3D microenvironment of the hydrogel scaffold can support mouse ESC self-renewal and proliferation activities. However, genetic background of mESCs altered the suitability of the hydrogel scaffolds to universally maintain all ESCs Thus, the mechanical properties of hydrogel scaffolds must be customized to support self-renewal of ESCs based on their genetic background. The inbred R1 and hybrid B6D2F1 ESCs showed the best self-renewal capacity in the 3D synthetic scaffolds with the mechanical properties provided by the 7.5% four-arm and 10% three-arm PEG-hydrogels, respectively. Determining an algorithmic pattern in response to genetic differences is important for developing customized 3D scaffolds for stem cell self-renewal or targeted differentiation.

These results indicate that the ECM has a pivotal role in ESC self-renewal. The positive actions of feeder cells on maintenance of stem cells *in vitro* can be partially replaced by a synthetic hydrogel scaffold. This important role of the ECM was also confirmed by comparing the results between the feeder-free and feeder-containing 2D and 3D systems. However, transcriptional expression of several self-renewal-related genes

differed between the hybrid and inbred ESC lines after 3D culture, which confirms results from previous studies(Lee et al., 2010, Lee et al., 2012, Jang et al., 2013). Understanding and controlling the ECM, niche, and/or microenvironment is important for regulating pluripotent cell function. Combined use of ESC culture and 3D synthetic scaffolds, as well as considering the genetic background of the ESCs, will greatly contribute to developing efficient practical stem cells.

CHAPTER 6

: Development of biomimetic microenvironment for human adipose derived stromal cell culture

1. Introduction

To construct biomimetic microenvironment for stem cells, it was important to analyze cellular characters and. Especially, cellular surface activity could be one of key component in cellular fate. Integrin heterodimer, cell surface receptors composed of non-covalently bonded α and β chain subunits, is a one type of signaling receptors for those extracellular stimuli and key factors for cell to cell or cells to extracellular matrix (ECM) communication. Stem cells selectively choose and use integrin subunits to active heterodimer form among total 18 types of α subunits and 8 types of β subunits depend on circumstance of cell, such as cell state like differentiation, proliferation, or even apoptosis (Huang et al., 1996, Hayashi et al., 2007). If this integrin mediated communication has been identified for each particular process, it could be helpful for controlling cell guided differentiation of ES cells by controlling integrin signal.

In stem cell culture system, constructing appropriate ECM is a one of key factors in maintaining cell proliferation and undifferentiated state of stem cells. ECM could be cellular or non-cellular in laboratory condition but originally cells were present at *in vivo* condition as a 3-dimentional, cellular microenvironment. However, in general, human stem cells were cultured in laboratory

condition with petri dishes and feeder cells which is far different from *in vivo* condition which were within living organism so it is important to reconstruct bio-mimicking 3-dimentional ECM in laboratory condition to understand and apply stem cells in direct research and practical use. In previous report, it was found that integrin directly recognize surrounding cells or extracellular proteins and following interaction alters depend on those materials. (Ellis and Tanentzapf, 2010) Therefore, precise analysis of integrin activity is necessary to construct appropriate cellular or non-cellular microenvironment for stem cells.

In this chapter, human adipose derived stromal cells (hADSCs) from human abdomen adipose from five random patient were employed as experimental cells. hADSCs share many cellular characters with human mesenchymal stem cells (hMSCs) and hMSCs were one of promising source of clinical researches such as tissue engineering or drug screening. (Liu et al., 2009)

To develop customized biomimetic microenvironment methods, stem cells from human origin was employed so the result could be compared with previous results. $CD31^{-}/45^{-}$ hADSCs were selected by MACS system and their integrin expression of were analyzed after MACS separation and after three subpassages of culture. Moreover, adhesive peptide sequence was conjugated to

suitable condition of PEG-based hydrogel to provide proper signal to encapsulated hADSCs. Fibronectin-originated RGD motif was choose as candidate adhesive peptide for $CD45^-/CD31^-$ hADSCs in this experiment

2. Material and Method

Experimental Design

As a first step of experiment, hADSCs were isolated from human abdomen adipose than immunomagnetically sorted with $CD45^-$ /$CD31^-$ hematopoietic/endothelial markers to get rid of hematopoietic/ endothelial cells. After sorting, Integrin expression of hADSCs were analyzed before primary culture of cells. Integrin expression of hADSCs were analyzed again after 3 culture passages than their expression were directly compared. In the second serious of experiment, effect of RGD peptide were tested. hADSCs were seeded into the polyethylene glycol (PEG)hydrogel with/without RGD peptide condition and their viability after 24 hours of seeding were observed. In the third series of experiments, hADSCs were seeded into the hydrogel with varied types (3, 4, and 8-arm) and concentrations [5%, 6.25%, 7.5%, 10.0%, 12.5% (wt/v)] of PEG hydrogel conjugated with adhesive peptide. The hADSCs were cultured in the designed 3D scaffolds for 14 days. hADSC proliferation and viability were measured on day 1, 7 and 14 of culture. In the next series of experiments, effect of RGD peptide concentration were monitored. hADSC proliferation and morphology

were measured on day 1, 7 and 14 of culture.

Experimental subjects and tissue samples

All protocols were reviewed and approved by the Seoul National University Institutional Review Board. To isolate ADSC, adult adipose tissues were obtained from five random patients who underwent gynecologic operation via laparotomy after receiving informed consent. Tissue samples were collected for study as follows: In the operation room, adipose tissues retrieved from visceral depots during surgery were immediately transferred into PBS containing FBS to isolate ADSC for further analysis.

Isolation and culture of adipose derived stromal cells.

Adipose tissue was washed in PBS to remove contaminating blood cells. Adipose tissue was cut and then connective tissue and blood vessel was removed. The specimen was minced, and digested with collagenase type IA (Sigma, St. Louis, MO, USA) for 1 hour at 37 ° C. The pellet was collected by centrifugation at 1500rpm for 4 minutes and then treated with RBC lysis buffer (Lonza, Barsel, Switzerland) for 5 minutes at room temperature to remove blood cells. After centrifugation, the pellet was filtered through 40 μm mesh filter. The filtrate was centrifuged, and MACS cell separation

(Miltenyi Biotec, Bergisch Gladbach, Germany) was performed with CD31, CD45, FCR antibodies (Miltenyi Biotec, Bergisch Gladbach, Germany) to isolate negative cells for CD31 (endothelial cell marker) and CD45 (hematopoietic cell marker), and the obtained cells was plated onto 100-mm culture dish in complete culture medium [1:1 Dulbecco's modified Eagle's medium-Ham's F-12 (DMEM/F12) containing 10% fetal bovine serum (FBS), 1% penicillin/streptomycin, 2mM L-glutamin, and 5ng basic fibroblast growth factor (bFGF)]. The cells were cultured at 37°C in humidified atmosphere with 5% CO2. After 3 days, nonadherent cells were removed. Confluent cells were trypsinized and expanded. Adipose-derived stromal cells (ADSC) were obtained by expansion of the adherent cells after passage 3.

Quantitative real-time polymerase chain reaction (PCR)

An RNeasy Mini Kit (Qiagen, Valencia, CA, USA) was used to extract total mRNA from ESCs, following the manufacturer's instructions, and cDNA synthesis from the extracted mRNA was conducted using a Superscript III first-strand synthesis system (Invitrogen, Carlsbad, CA, USA). Quantification of gene expression was performed using iQ SYBR Green Supermix (Bio-Rad

Laboratories, Hercules, CA, USA) in a Bio-Rad iCycler iQ system (Bio-Rad Laboratories). Data on melting curves were collected to check PCR specificity and the β-actin gene was used as an internal control to normalize specific gene expression. mRNA levels were calculated as $2^{-\Delta Ct}$, where Ct = threshold cycle for target amplification and $\Delta Ct = Ct_{\text{target gene}}$ (specific genes for each sample) $- Ct_{\text{internal reference}}$ (β-*actin* for each sample). Supplementary Table 1 provides general information and sequences for all specific primers designed with mouse cDNA sequences obtained from GenBank using Primer3 software (Whitehead Institute/MIT Center for Genome Research).

Flow cytometry

The hADSCs were washed with ice cold Dulbecco's phosphate buffered saline (DPBS; Gibco Invitrogen). Then the ESCs were stained for 30 min at 4° C with PE-conjugated anti-human integrin α_5, α_6, α_9, and α_V, FITC-conjugated anti-human integrin β_1, β_4, β_5, and β_5, and fluorescence-unconjugated anti-mouse integrin α_8 antibodies. The fluorescence-unconjugated primary antibody was detected by incubation with Alexa Fluor 488-conjugated anti-rabbit IgG. All antibodies were diluted in DPBS

supplemented with 2% (v/v) heat-inactivated FBS. Supplementary Table 2 provides detailed information and dilution rates of primary and secondary antibodies. The stained cells were washed and sorted using flow cytometry with a CyAn ADP Analyzer (Beckman Coulter, Inc., Fullerton, CA, USA). The FLOWJO Ver. 7.2.5 software program (Tree Star, Inc., Ashland, OR, USA) was used to analyze acquired data.

Formation of PEG-based hydrogel, encapsulation of ESCs into poly(ethylene glycol) (PEG)-based hydrogel and culture

Vinylsulfone (VS; Sigma-Aldrich)-functionalized 3-arm, 4-arm and 8-arm PEG (PEG-VS) were synthesized as previously described and dicystein-containing peptides with an intervening matrix metalloproteinase (MMP)-specific cleavage site (Ac-GCRD-GPQGIWGQ-DRCG-NH2) were used as crosslinker connecting among PEG-VS(Lutolf et al., 2001). Moreover, according to previously described protocols (Lee et al., 2010), construction of the PEG-based hydrogel, incorporation of cell adhesion peptides to the PEG-based hydrogel and encapsulation of ADSCs into the hydrogel were performed. Subsequently, ADSCs encapsulated into the hydrogel were cultured in standard ADSCs

culture medium at 37° C in a humidified atmosphere of 5% CO_2 in air and replacement of medium was conducted every day. The cultured ADSCs were retrieved from the hydrogel by incubating in 10 mg/ml collagenase I (Sigma-Aldrich) solution for 10 minutes and enumerated using a hemocytometer.

Adhesion peptide synthesis and purification

Synthesis and purification of adhesion peptides were conducted as previously described(Lutolf et al., 2001, Lutolf and Hubbell, 2003). Briefly, an automated peptide synthesizer (PerSpective Biosystems, Farmington, MA) adjusting standard Fmoc/HBTU/HOBT chemistry was used for synthesizing adhesion peptides and C18 chromatography (Biocad 700E; PerSpective Biosystems) was used for purifying synthesized adhesion peptides. Subsequently, identification of synthetic adhesion peptide sequences of AcGCGWGRGDSPG was conducted by matrix-assisted laser desorption ionization/time-of-flight (MALDI-TOF) mass spectrometry.

Monitoring of proliferation activity

Cell viability was represented by absorbance measured by a CCK or BRDU assay. On 1 day and 7, 14 days of culture, the cell counting kit (CCK)-8 reagent (Dojindo Laboratories, Kumamoto, Japan) was added to each well containing a variety of the hydrogels encapsulating ADSCs. After 3 hours of incubation, the absorbance of CCK-8 was measured at 450 nm using Bio-Rad microplate reader Model-550 (Bio-Rad Laboratories, Hercules, CA). Subsequently, proliferation activity of ADCs was calculated as $A_{(day7, day14)}/A_{day1}$, where $A_{(day7, day14)}$ = absorbance on day 7, 14 of culture, and A_{day1} = absorbance on day 1 of culture. As a same protocol, BRDU proliferation assay kit (Roche, Swiss) was used to measure cell proliferation. On 1 day and 7, 14 days of culture, cell culture medium was replaced with BRDU assay solution in each wells containing hydrogels. After 3 hours of incubation, BRDU solution and encapsulating hydrogels were removed without cells. The absorbance of BRDU was measured at 450 nm using Bio-Rad microplate reader Model-550 (Bio-Rad Laboratories, Hercules, CA).

Monitoring of Live/Dead status of ADSCs

On 1 day of culture within hydrogel, the Live/Dead assay kit (Invitrogen) was used to washed well containing a variety of the hydrogels encapsulating ADSCs. Calcein AM solution was added to each washed hydrogels to stain live cells and Ethidium homodimer-1(EthD-1) solution was added to stain dead cells. After 45 minuts of stainig, hydrogels were washed with PBS and Live/Dead cells nd observed under Nikon Eclipse TE2000-U microscope (Nikon) equipped with a JENA ProgRes camera (JENOPTIK).

Statistical analysis

All the numerical data derived from each experiment were analyzed in the Statistical Analysis System (SAS) program. Moreover, when a significant main effect was detected by analysis of variance (ANOVA) in the SAS package, the least-square or DUNCAN methods were used for comparison among treatments. Differences among treatments were considered significant when the p value was less than 0.05.

Table 8. Oligonucleotide primers and PCR cycling conditions of human integrin subunits.

Genes	GenBank number	Primer sequence		Size (bp)	Temp
		Sense (5' >3')	Anti-sense (5' >3')		
Actb	NM_001101	AGAGAAGTGGGGTGGCTTTT	AAACTGGAACGGTGAAGGTG	200	60
Ita1	NM_181501	AAGATGATCACGGGGGAGCTG	ACCACCAAGGCCCCCAATAGT	200	60
Ita2	NM_073107	TGGCTGGAGTGGGACCATTG	GGCCGGTATAATTTGCCCGA	181	60
Ita3	XR_001752507	GCCCACTCACTGCCCACAAG	GCCGCTGGTCTTCTGACCCT	158	60
Ita4	NM_001316312	GAGAGCGCGCTGCTTTACCA	CGTCTGGCCGGGATTCTTTC	160	60
Ita5	XM_02448970	AACCCAGAGGAGCGGAGCTG	GCCTGGAGGCCAGGAACAGT	178	60
Ita6	XM_017004008	CAAGCGGCTGTTGCTCGTG	GACGGTGACCCCCATCCACT	185	60
Ita7	XM_005268842	TAGCACCTCCGGGATCAGCA	CTCTCTCGCCCCTCACCACA	182	60
Ita8	XM_011519752	GCATTCTTGACGTGGGCTGG	TCCGTCTGCTTTTCTCCTGCC	154	60
Ita9	NM_002207	GCGCAGTTGACCTGAATGGG	GGCTGGCAATGCTCTCTCCA	156	60
Ita10	XM_017002628	CCAGAGTGGAGTCAGGCCCC	GTCAGATGGACAATGGGCCG	186	60
Ita11	XM_005254228	CTGGAACGGCTGCAATGAGG	ACTCGCTGGCGTGTGCTCTC	172	60
Itav	NM_001145000	TTCCATTCCACTGCAGGCTGA	TGCTGGTGCACACTGAAACGA	194	60
Ital	XM_024450262	TGCTGAAGCCCCATAGCCAG	GCAATTCAACCGAGTCCCCC	180	60
Itam	XM_011545850	AGCAACCTGGGGCAGAGGAG	CCTTCCGAAGCTCAGCCAGAA	150	60
Itad	XM_011545848	TGTCCGTGTGTCCCTTGCCT	CACCCCGGTTCTCCTGCTCT	157	60
Itax	XR_950797	TTACATACACGGCCACCGCC	GCATAGCGGATGATGCCTGC	165	60
Itae	XM_011523828	GGGGGCTCCACGGTACAAAC	AATGGAGCAGCCACCAGCAA	186	60
Itb1	NM_002211	TGCAAGAACGGGGTGAATGG	CCTCCGTAAAGCCCAGAGGC	167	60
Itb2	XM_006724001	GCGTTCAACGTGACCTTCCG	TTGTCCACGAAGGACCCGAA	165	60
Itb3	NM_000212	CAGCATTGAGGCCAAGGTGC	ACCCCACACTCAAAGGTCCCA	166	60
Itb4	XM_006721870	CTGGATGCTCCTGAGGGCG	TCCAGGTGGCACCGTTCATC	151	60
Itb5	XM_017006354	TCCAAATTGCGTCCCCTCCT	CAGTGCATCCTTTCGCCAGC	161	60
Itb6	NM_001282390	GCAAGGAGGCCCCAGATCAT	CACCACAGTCACAGTCGCCG	199	60
Itb7	XR_429099	AACGGTGCTGCCCTTTGTGA	AGCCACCTTCAGGCGAGTCC	182	60
Itb8	XM_017012183	TCTTGCCAGGCACCATTGCT	TCCATGCCTGGCTTTCTGGA	181	60

Ita=integrin α, Itb=integrin β

Table 9. Primary and Secondary Antibodies of human surface integrin.

Antibody Name	Catalog Number	Company	Application	Dilution Rate
PE-conjugated anti-human integrin α_1	FAB8624P	R&D systems	FACS[a]	1:100
PE-conjugated anti-human integrin α_2	FAB1233P	R&D systems	FACS[a]	1:100
PE-conjugated anti-human integrin α_4	FAB1354P	R&D systems	FACS[a]	1:100
PE-conjugated anti-human integrin α_5	12-4900-41	Thermo	FACS[a]	1:100
PE-conjugated anti-human integrin α_6	FAB13501P	R&D systems	FACS[a]	1:100
anti-human integrin α_7	LS-C313325	LifeSpan	FACS[a]	1:100
anti- human integrin β_1	MAB17781	R&D systems	FACS[a]	1:100
FITC-conjugated anti-human integrin β_3	Ab92393	abcam	FACS[a]	1:100
FITC-conjugated anti-human integrin β_5	11-0497-41	eBioscience	FACS[a]	1:100
PE-conjugated goat anti-rabbit IgG (H+L)	Ab72465	abcam	FACS[a]	1:100
APC-conjugated goat anti-rabbit IgG (H+L)	A-865	Thermo	FACS[a]	1:100

[a]FACS=Fluorescence-activated Cell Sorting

3. Results

Transcriptional and translational expression of integrin subunits in $CD45^{-}CD31^{-}$ human adipose derived cells (ADSCs) before primary culture .

In this experiment, both transcriptional and translational expressions of $\alpha 2$, $\alpha 5$, $\alpha 9\beta 1$, αv, $\beta 1$, $\beta 5$ integrin subunits were detected in $CD45^{-}/CD31^{-}$ hADSCs, which could be matched with fibronectin, vitronectin or laminin. Among total 17 integrin α and 8 integrin β subunit genes, real-time PCR showed that transcriptional levels of 10 α and 1 β subunit genes were increased significantly in non-cultured cells, (Fig.11) and α_5, α_7 and β_1 subunit genes were increased in cultured cells. (Fig.13) The translational levels of integrin α_5, $\alpha_9\beta_1$, α_v, β_1, β_5 were identified in non-cultured cells, (Fig.12) and α_2, α_5, α_v and β_1 were detected in cultured cells by fluorescence activated cell sorting (FACS). (Fig.14)

a

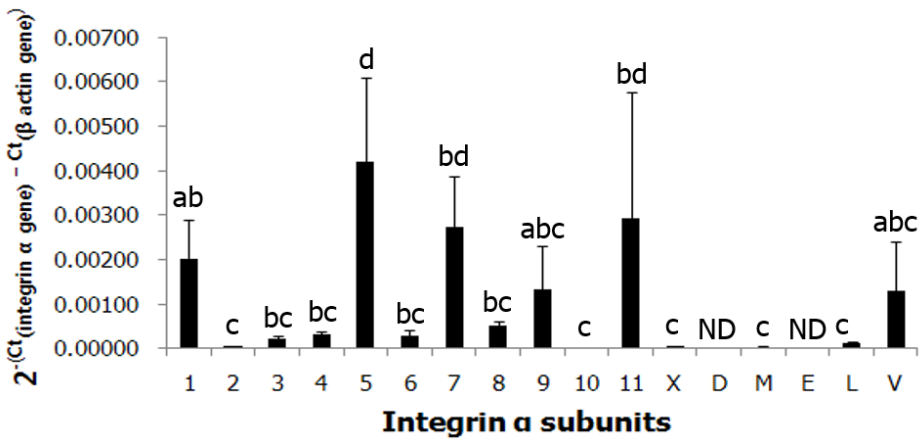

b

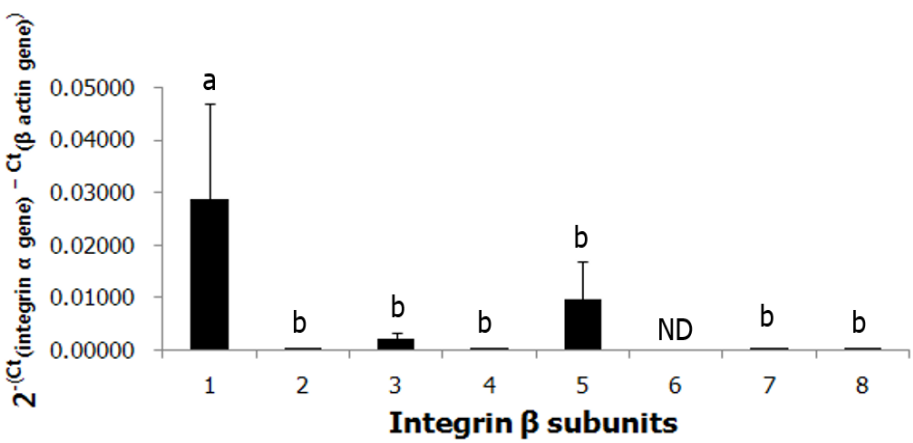

Figure 11. Transcriptional expression of integrin subunits in CD45$^-$CD31$^-$ human adipose derived stromal cells (ADSCs) before primary culture. ADSCs were isolated from human adipose tissue and then CD45$^-$CD31$^-$ cells were separated using magnetic activated cell sorting (MACS). Transcriptional level of integrin α (a) and β (b) subunit genes were observed immediately after CD45$^-$CD31$^-$ cell sorting. $^{a, b, c, d}$ $P < 0.05$ and ND=not detected.

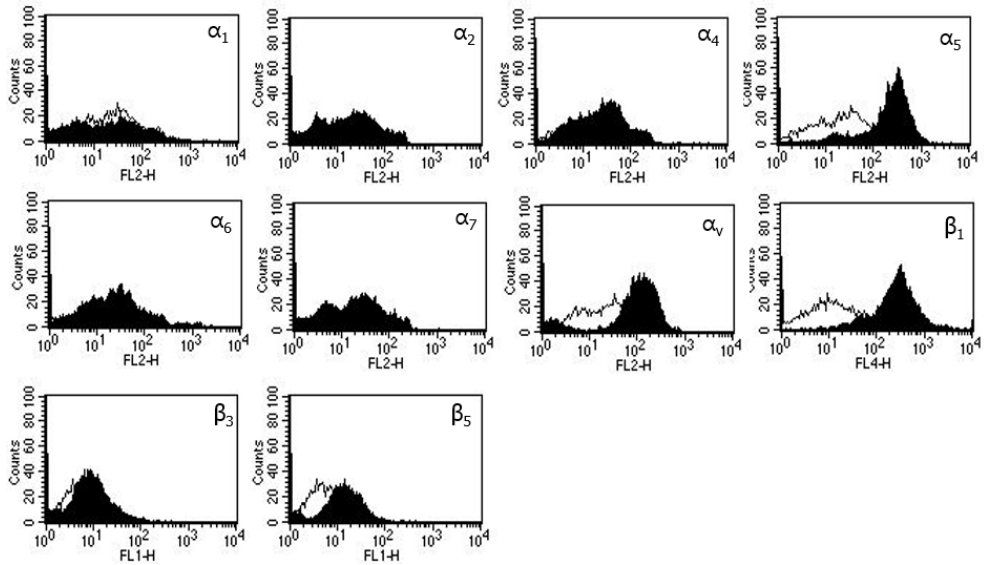

Figure 12. Translational expression of integrin subunits in $CD45^{-}$ $CD31^{-}$ human adipose derived stromal cells (ADSCs) before primary culture. ADSCs were isolated from human adipose tissue and then $CD45^{-}CD31^{-}$ cells were separated using magnetic activated cell sorting (MACS). translational level of integrin α and β subunit genes were observed immediately after $CD45^{-}CD31^{-}$ cell sorting.

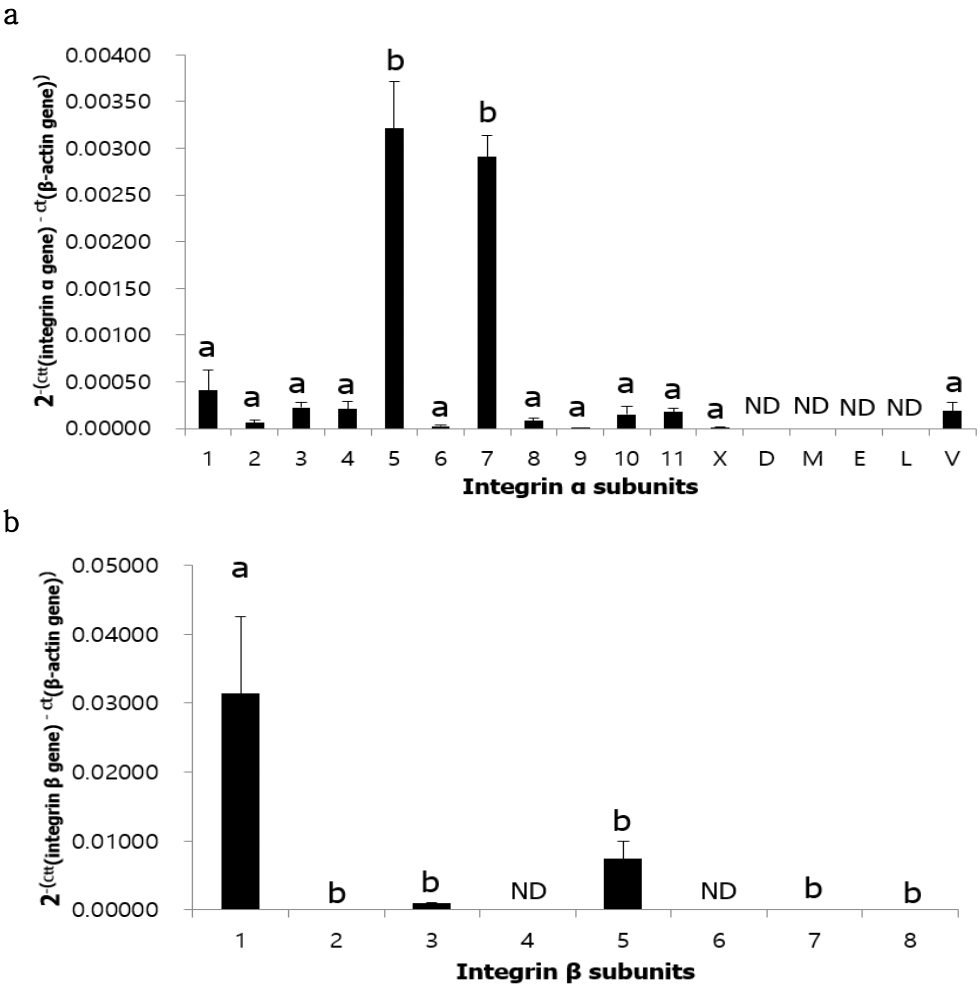

Figure 13. Transcriptional expression of integrin subunits in $CD45^{-}$ $CD31^{-}$ human adipose derived stromal cells (ADSCs) after cell culture. Transcriptional level of integrin α (a) and β (b) subunit genes were observed immediately after culturing for three culture passages. $^{a, b, c, d}$ $P < 0.05$ and ND=not detected.

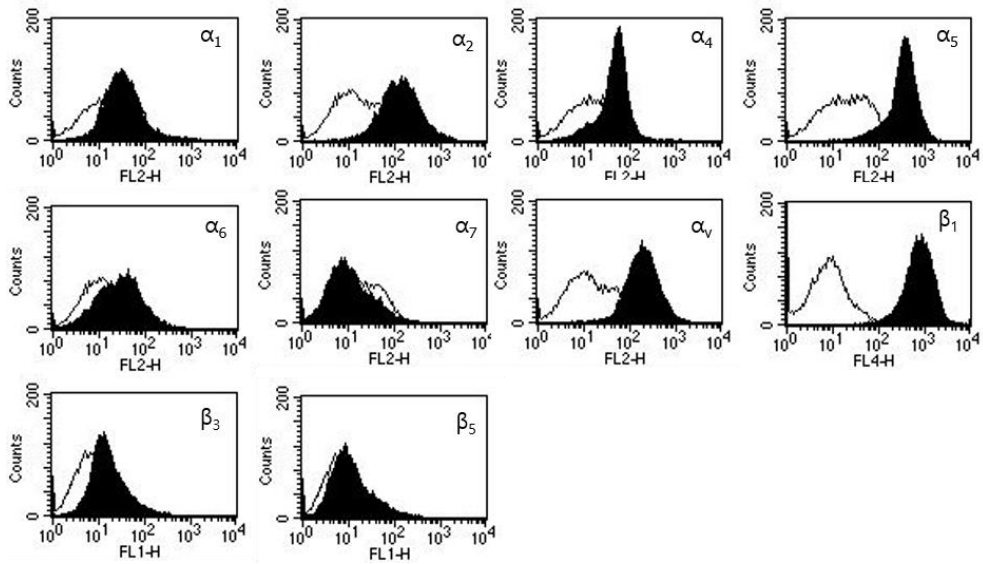

Figure 14. Translational expression of integrin subunits in $CD45^{-}$ $CD31^{-}$ human adipose derived stromal cells (ADSCs) after cell culture. Translational level of integrin α and β subunit were observed immediately after culturing for three culture passages.

Effect of fibronectin originated RGD motif in encapsulation of human adipose derived stromal cells (hADSCs) into polyethylene-glycol (PEG) hydrogel.

In this experiment, effect of RGD motif in cell viability at 3D extracellular matrix was confirmed. $CD45^{-}/CD31^{-}$ hADSCs were cultured in 3D extracellular matrix showed better cell viability at day 1 of culture with 400 μM of fibronectin-originated RGD motif attached PEG hydrogels than no RGD motif group. With Calcein AM (live-green) and EthD (dead-red) uptake condition, more lived cells and less number of dead cells could be observed in 400 μM of fibronectin-originated RGD motif attached group. RGD motif enhanced cell attachment by activating integrin heterodimers and proliferation of the hADSCs (Fig. 15)

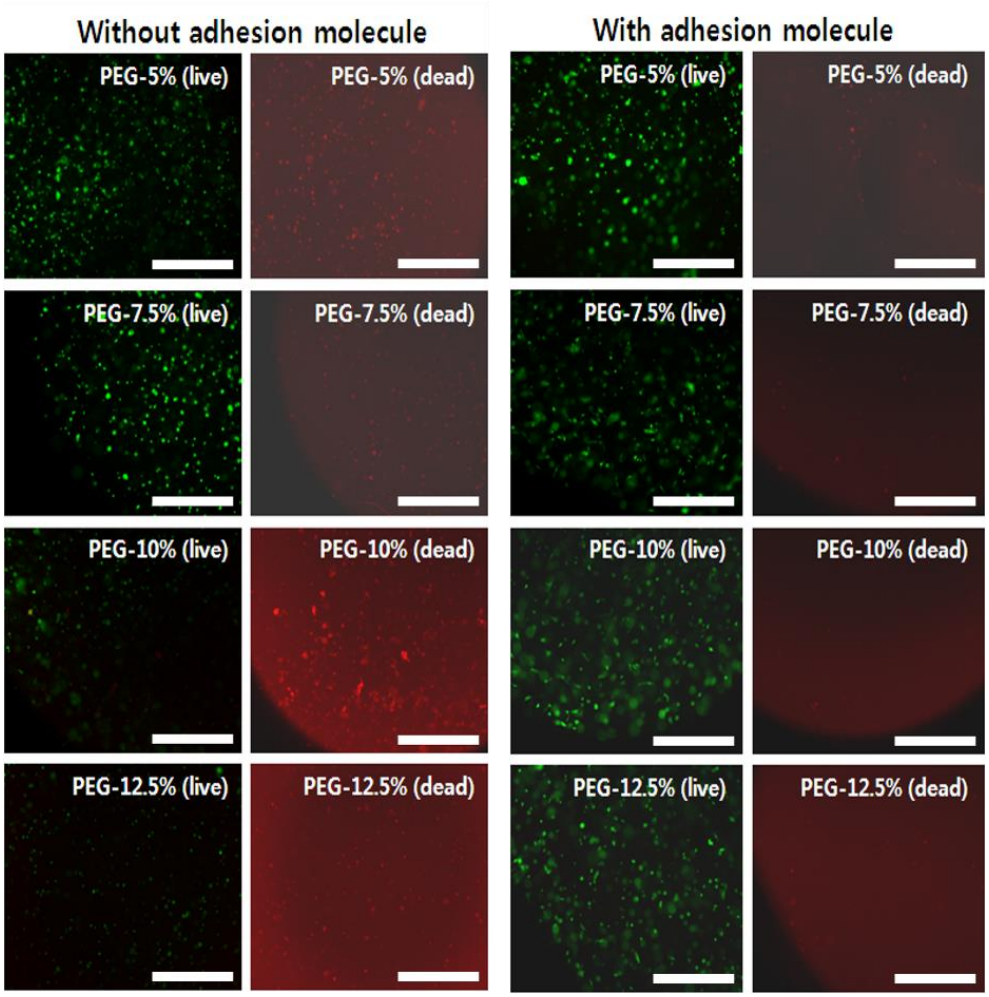

Figure 15. Effect of fibronectin originated RGD motif in encapsulation of human adipose derived stromal cells (hADSCs) into polyethylene-glycol (PEG) hydrogel. The PEG hydrogels of 5%, 7.5%, 10% or 12.5% were conjugated with vinylsulfone (VS)-functionalized four-arm PEG hydrogels with 400 μM fibronectin RGD motif peptide. The Calcein AM (live-green) and EthD (dead-red) uptake was monited by fluorescence image analyzer on the day 1.

Effect of mechanical properties of polyethylene-glycol (PEG) gel on human adipose derived stromal cells (hADSCs).

In this experiment, hADSCs were cultured in 5, 7.5, 10 or 12.5% concentration of 3, 4 or 8 vinyl sulfone-functionalized multiarms PEG hydrogels with 400μM of RGD motif. Cell proliferation activity of hADSC was monitored with brdU analysis on day 1, 7 and 14. Overall, a 3-arm PEG hydrogel conjugated in 5%, 7.5%, 10% or 12.5% PEG hydrogel yielded better proliferation of hADSCs. Among different concentration of conjugation, 5% PEG hydrogel showed best cell proliferation in all types of PEG hydrogel. (Fig.16)

a

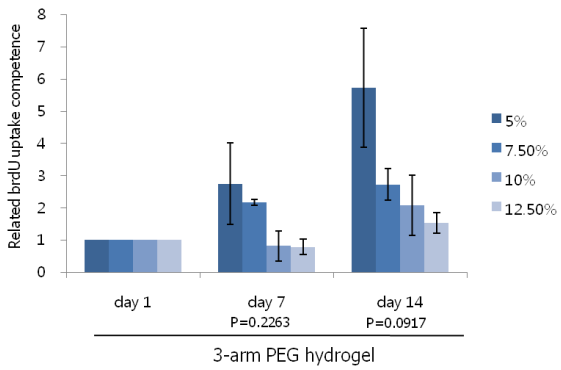
Related brdU uptake competence
8
7
6
5
4
3
2
1
0
5%
7.50%
10%
12.50%
day 1
day 7
P=0.2263
day 14
P=0.0917
3-arm PEG hydrogel

b

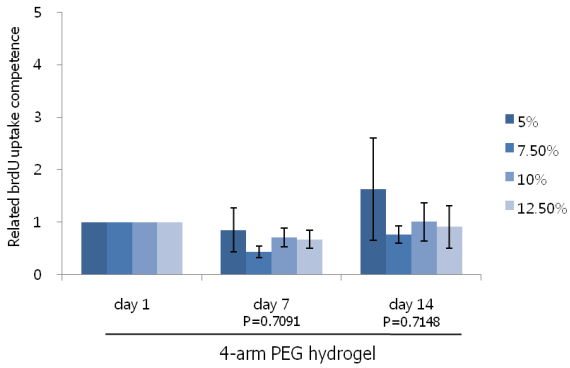
Related brdU uptake competence
5
4
3
2
1
0
5%
7.50%
10%
12.50%
day 1
day 7
P=0.7091
day 14
P=0.7148
4-arm PEG hydrogel

c

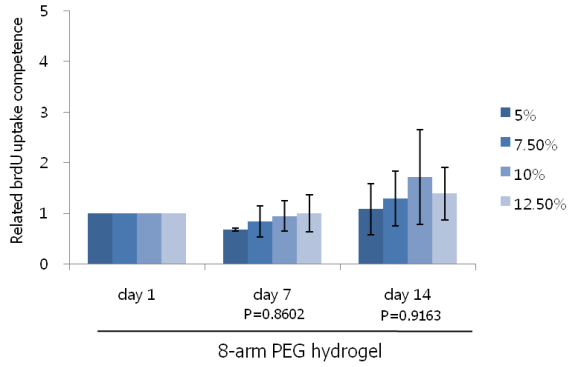
Related brdU uptake competence
5
4
3
2
1
0
5%
7.50%
10%
12.50%
day 1
day 7
P=0.8602
day 14
P=0.9163
8-arm PEG hydrogel

Figure 16. Effect of mechanical properties of polyethylene-glycol (PEG) gel on BrdU uptake competence of human adipose derived stromal cells (hADSCs). The PEG gel of 5%, 7.5%, 10% or 12.5% which consisted of vinylsulfone (VS)-functionalized multi-arm PEG derivatives including 3-, 4- or 8-arm with 400μM fibronectin RGD motif peptide. The BrdU uptake competence was measured by multilabel plate reader on the day 1, day 7, day 14 of culture. The relative BrdU uptake competence of (a) 3arm PEG gel (b) 4arm PEG gel (c) 8arm PEG gel. All data shown were means $\pm$ S.E.

Effect of mechanical properties of polyethylene-glycol (PEG) gel on cell proliferation of human adipose derived stromal cell (ADSCs).

The hADSCs cultured in 5% 3-arm PEG showed increased cell growth than other PEG concentrations. However, 5% PEG hydrogel had critical disadvantage to manipulate and to maintain stable cell proliferation. After 14 days of culture, many hydrogels in 5% 3-arm PEG lysed into culture media which could make difficulties in analyzing results. The 6.25% PEG hydrogel were tested to substitute 5% hydrogel and yielded similar proliferation compared with the 5% PEG hydrogel, which efficiently, eliminated the disadvantages observed in the 5% PEG. No significant effect of arm number was detected in both PEG concentrations in each PEG concentration, while 3-arm yielded better results. (Fig.17)

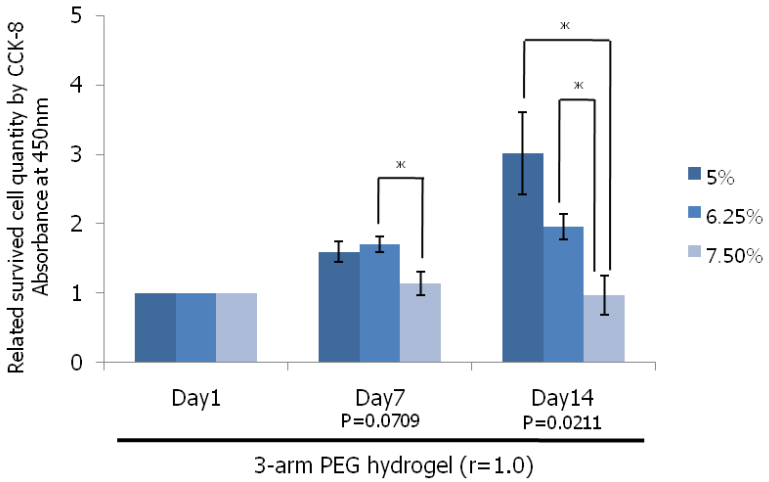

Figure 17. Effect of mechanical properties of polyethylene-glycol (PEG) gel on Cell Count Kit-8 (CCK-8) uptake competence of human adipose derived stromal cell (ADSCs) of 3arm PEG gel. The PEG gel of 5%, 6.25%, or 7.5% which consisted of vinylsulfone (VS)-functionalized 3-arm PEG with 400 μM fibronectin RGD motif peptide. The related CCK-8 uptake competence was measured by multilabel plate reader on the day 1, day 7, day 14 of culture. $^{*}P<0.05$ between two comparison groups. All data shown were means ± S.E.

Effect of fibronectin originated RGD motif in proliferation of human adipose derived stromal cells (hADSCs) within polyethylene-glycol (PEG) hydrogel.

In this experiment, 0, 200, 400, 800 or 1,200 μM RGD motif was employed in the culture of hADSCs in a 6.25% PEG hydrogel with 3-arm PEG hydrogels. Increased proliferation of encapsulated hADSCs in a dose response manner up to 400 or 1,200 μM RGD motif was detected. After 7 days of culture, 400, 800 and 1,200 μM RGD containing group showed significant difference with 0, 200 μM RGD containing group, and after 14 days of culture, all RGD motif containing group showed significant increase of cell quantity than no RGD motif group and showed dose response within RGD motif containing group. Moreover, morphological changes also founded in RGD contraining group. hADSCs stretched their branches when they were in RGD containing hydrogels. (Fig.18)

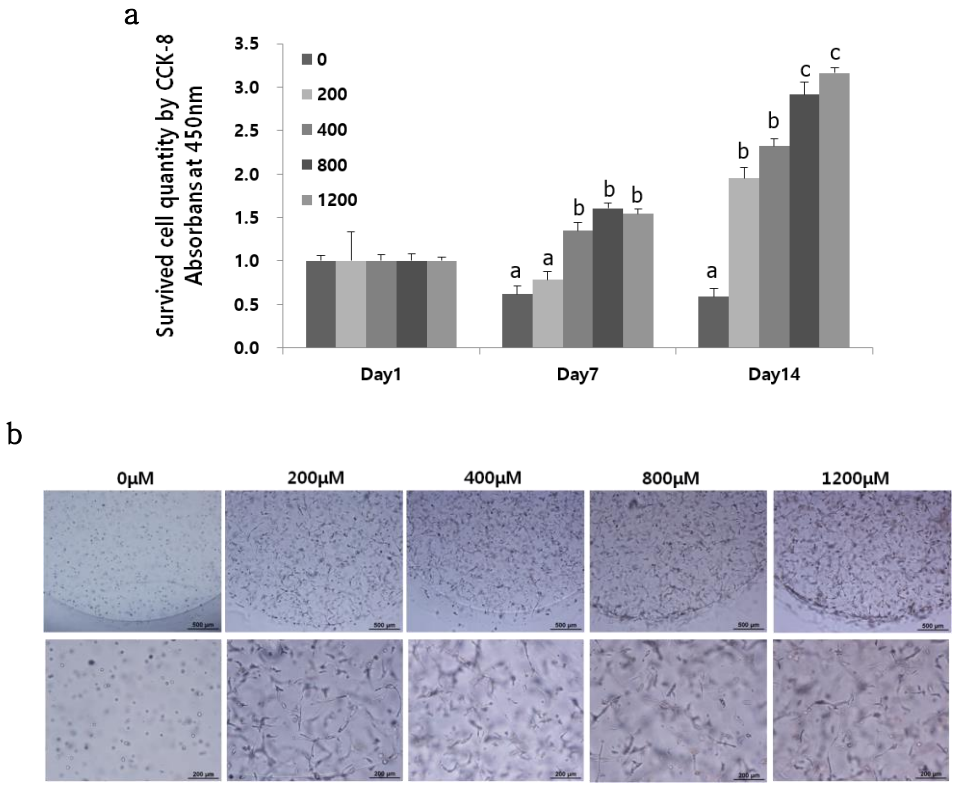

Figure 18. Proliferation of adipose derived stromal cells (ADSCs) in polyethylene glycol (PEG) hydrogel. ADSCs were cultured in different concentration of RGD containing PEG hydrogel. Proliferation was detected using Cell Counting Kit 8 (CCK8) kit at day 1, day 7 and day 14 (a). Morphology of the cells was observed 20 days after culturing in PEG hydrogel with different concentration of RGD (b).

4. Discussion

From the results of this chapter, possible candidate of integrin heterodimers were integrin $\alpha_5\beta_1$ and $\alpha_v\beta_1$. These integrin heterodimers both known as interact with fibronectin. With this information, it could be able to establish hADSCs specific biomimetic environment establishment methods if this results combined with microenvironment establishment methods of previous chapter.

After few passages of culture, results for integrin screening were obviously stabilized in hADSCs. Primary culture and MACS separation allows to stabilize hADSCs to use in research process. To construct proper microenvironment for stem cell, microenvironment should interact with stem cell properly by their integrin heterodimers. Self-renewal and cell proliferation, differentiation, and other many cellular fate were depend on their surrounding microenvironment. To apply stem cells into other applications fields, role of human surface integrin in 3D microenvironment should be researched.

The results of this study provide proper condition of biomimetic microenvironment for hADSCs culture. Significantly higher proliferation rate was observed in 3-arm 6.25% of PEG hydrogel which is conjugated with RGD motif peptide. It was clear

that PEG types and their concentration, type of adhesion peptide and their amount were key component in making proper microenvironment . these factors directly influence cellular activity of encapsulated ADSCs.

hADSCs from random patients may not represent general compatibility for every human individuals in further application. However, this study could provide general methods and parameters to develop patient-specific stem cell culture condition for biomimetic culture system.

CHAPTER 8

: General Discussion & Conclusion

Based on these experiments, the general methods for constructing stem cell-specific 3D culture systems were described. In general, stem cells were cultured under laboratory conditions in petri dishes with feeder cells as in 2D systems, which are far different from the *in vivo* conditions in live organisms. It is therefore important to reconstruct biomimetic 3D culture systems in the laboratory, to better understand and apply stem cells for both basic research and clinical use. Furthermore, development of an artificial stem cell ECM for 3D culture systems could facilitate a better understanding of cell-ECM interactions.

The expansion of cellular resources for ESCs could provide a better infrastructure for stem cell research. In Chapter 3, optimal oocyte collection methods were used to obtain quality oocyte-ESC precursor cells from young and aged mice. The proper types of gonadotropins were confirmed to be present in large amounts in the oocytes of all mice, and the adverse effects on developmental competence in aged mice were characterized in this chapter.

In Chapters 4 and 5, the optimal conditions for artificial scaffolds suitable for specific types of mESCs were developed. It was assumed that each different cell type requires a customized microenvironment for 3D culture. In previous studies from this laboratory, typical mESCs showed phenotypic changes in a

synthetic microenvironment optimized to culture other types of mESCs. Two different types of mESCs, inbred R1 and hybrid B6D2F1, were tested in various types of hydrogels and cell surface interactions to optimize hydrogel conditions, followed by analyses of cellular reactivities in these hydrogels. (Lee et al., 2016)

In Chapter 4, screening of functional integrins on the surface of mESCs was conducted to adjust the biochemical properties of artificial scaffolds. In this study, inbred R1 and hybrid B6D2F1 ESCs showed similar expressions of functional integrins, and $\alpha_6\beta_1$ and $\alpha_v\beta_1$ integrins were identified in both strains of mouse ESCs when they were cultured in a conventional 2D culture system in their undifferentiated states.

In Chapter 5, suitable mechanical properties of 3D synthetic scaffolds for mouse ESC culture were evaluated. A synthetic niche maintaining self-renewal of inbred E14 ESCs did not show any universality against inbred R1 and hybrid B6D2F1 ESCs in the maintenance of ESC self-renewal. Subsequently, in trials for establishing synthetic ECM scaffolding customized to the genetic background of ESCs in the self-renewal of ESCs, inbred R1 and hybrid B6D2F1 ESCs showed the best self-renewal inside the 3D synthetic scaffold with mechanical properties derived from 7.5% (w/v) 4-arm and 10% (w/v) 3-arm PEG hydrogel, respectively.

From these results, the dependence of niche composition supporting a specific property of ESCs on the genetic backgrounds of ESCs was identified, to simultaneously provide the basis for completing genetic background-specific synthetic niches engineered with ECM analogs.

In these experiments, different types of mESCs from different genetic backgrounds showed different results in supporting self-renewal and the undifferentiated state of mESCs. The R1 ESC line and B6D2F1 ESC line showed different behaviors under different types of 3D culture conditions. For the R1 ESC line, the highest cell proliferation was observed with 7.5% (w/v) 4-arm PEG-based hydrogel, and their mRNA expression showed upregulated transcription of self-renewal-specific genes. However, for the B6D2F1 ESC line, cells in 10.0% (w/v) 3-arm PEG-based hydrogels showed the highest cell proliferation, and their mRNA expression showed relatively lower transcription of self-renewal-specific genes compared with those in 2D culture or those of R1 ESC lines.

As a result, the R1 and B6D2F1 ESC lines showed different patterns of mRNA expression when cultured using the customized synthetic extracellular matrices. With these results, we were able to infer the supporting capacity for self-renewal of 3D synthetic

matrices when applied differently to different types of mouse ESCs. There were two possible reasons to explain the above differences. First, different mechanical properties of synthetic niches could result in different reactivities of mESCs. A previous study reported that hydrogel stiffness surrounded embedded cells, influencing integrin-cell interactions (Sanz-Ramos et al., 2012). The 7.5% (w/v) 4-arm hydrogel and 10.0% (w/v) 3-arm hydrogel were different in arm number and concentration of PEG-VS, and should thus have different mechanical properties such as stiffness of the hydrogel. This could cause different types of signal transduction pathway events, which could alter integrin interactions. Second, the different genetic backgrounds of inbred R1 and hybrid B6D2F1 ESCs may lead to the above differences. A previous study reported that genetic variation in mouse strains was responsible for the integrin reactivity of cells with ECM. (Li et al., 2004) This might also play an important role in integrin-triggered signal transduction pathways, which might influence the self-renewal capacity of the synthetic niche. These proposed explanations could be verified by attaching adhesion molecules to a synthetic niche (such as RGDSP) or by blocking integrin heterodimers in mESCs using blocking antibodies.

For the next study, general methods to establish a biomimetic microenvironment for hADSCs were developed. To test the clinical feasibility of 3D culture systems, hADSCs were selected to test cellular reactivity in such a system. General development of methods for isolating ADSCs and constructing the microenvironment for hADSCs are discussed in Chapter 6. For the first experiments, transcriptional and translational analyses of integrins on the surface of hADSCs were conducted to adjust the biochemical properties of the artificial scaffolds. In the present study, CD45−/CD31 hADSCs showed different expression of integrin subunits depending on their status. Non−cultured isolated hADSCs showed different aspects of transcriptional expression of integrins. However, at the translational level, both cultured and non−cultured hADSCs expressed the integrins α_5, α_v, and β_1. Based on these results, the fibronectin−originated rat genome database (RGD) motif peptide was selected as an adhesive peptide for the next step of the experiment, which involved the evaluation of suitable mechanical properties and the amount of adhesive peptides in 3D synthetic scaffolds for hADSC culture. Cell survival and proliferation of hADSCs were evaluated in various conditions of PEG and adhesive peptides. For hADSCs, 6.25% 3−arm PEG hydrogel conjugated with the RGD motif peptide showed

significantly higher cell proliferation.

In these studies, three different cell lines were directly compared in constructing a 3D culture system. Each cell line tested, including two similar cell lines (two types of mESCs) and one totally different cell line (hADSCs), required different optimal 3D culture conditions. Even the two types of mESCs from different genetic backgrounds, which showed similar integrin expression in conventional 2D culture conditions, showed different behaviors when adjusting to 3D culture conditions; thus, hADSCs also needed separate culture conditions.

On a structural basis, it is clear that a 3D culture system is superior to a 2D system. The 3D culture systems improved cell–cell/cell–ECM interactions, and their structural properties mimicked the *in vivo* 3D structure. Overall, recent studies have indicated that the transition from 2D to 3D cell culture systems shows promising clinical applications, by bridging 2D cultures to 3D systems that more realistically mimic the *in vivo* environment of cells.

REFERENCES

AKSU, A. E., RUBIN, J. P., DUDAS, J. R. & MARRA, K. G. 2008. Role of gender and anatomical region on induction of osteogenic differentiation of human adipose-derived stem cells. *Ann Plast Surg,* 60, 306-22.

AUERBACH, A. B., NORINSKY, R., HO, W., LOSOS, K., GUO, Q., CHATTERJEE, S. & JOYNER, A. L. 2003. Strain-dependent differences in the efficiency of transgenic mouse production. *Transgenic research,* 12, 59-69.

AVILION, A. A., NICOLIS, S. K., PEVNY, L. H., PEREZ, L., VIVIAN, N. & LOVELL-BADGE, R. 2003. Multipotent cell lineages in early mouse development depend on SOX2 function. *Genes Dev,* 17, 126-40.

BAHARVAND, H. & MATTHAEI, K. I. 2004. Culture condition difference for establishment of new embryonic stem cell lines from the C57BL/6 and BALB/c mouse strains. *In Vitro Cell Dev Biol Anim,* 40, 76-81.

BIRBRAIR, A. & FRENETTE, P. S. 2016. Niche heterogeneity in the bone marrow. *Ann N Y Acad Sci,* 1370, 82-96.

BRADLEY, A., EVANS, M., KAUFMAN, M. H. & ROBERTSON, E. 1984. Formation of germ-line chimaeras from embryo-derived teratocarcinoma cell lines. *Nature,* 309, 255-6.

BRIZZI, M. F., TARONE, G. & DEFILIPPI, P. 2012. Extracellular matrix, integrins, and growth factors as tailors of the stem cell niche. *Curr Opin Cell Biol,* 24, 645-51.

BROOKE, D. A., ORSI, N. M., AINSCOUGH, J. F., HOLWELL, S. E., MARKHAM, A. F. & COLETTA, P. L. 2007. Human menopausal and pregnant mare serum gonadotrophins in murine superovulation regimens for transgenic applications. *Theriogenology,* 67, 1409-13.

BRYANT, S. J., BENDER, R. J., DURAND, K. L. & ANSETH, K. S. 2004. Encapsulating chondrocytes in degrading PEG hydrogels with high modulus: engineering gel structural changes to facilitate cartilaginous tissue production. *Biotechnol Bioeng,* 86, 747-55.

BRYJA, V., BONILLA, S., CAJANEK, L., PARISH, C. L., SCHWARTZ, C. M., LUO, Y., RAO, M. S. & ARENAS, E. 2006. An efficient method for the derivation of mouse embryonic stem cells. *Stem Cells,* 24, 844-9.

BYERS, S. L., PAYSON, S. J. & TAFT, R. A. 2006. Performance of ten inbred mouse strains following assisted reproductive technologies (ARTs). *Theriogenology,* 65, 1716-26.

CAMPOS, L. S. 2005. Beta1 integrins and neural stem cells: making sense of the extracellular environment. *Bioessays,* 27, 698-707.

CHAMBERS, I., COLBY, D., ROBERTSON, M., NICHOLS, J., LEE, S., TWEEDIE, S. & SMITH, A. 2003. Functional expression cloning of Nanog, a pluripotency sustaining factor in embryonic stem cells. *Cell,* 113, 643-55.

CHOI, J. K., AHN, J. I., PARK, J. H. & LIM, J. M. 2011. Derivation of developmentally competent oocytes by in vitro culture of preantral follicles retrieved from aged mice. *Fertility and sterility,* 95, 1487-9.

DAVIS, F. F. 2002. The origin of pegnology. *Adv Drug Deliv Rev,* 54, 457-8.
DOMOGATSKAYA, A., RODIN, S., BOUTAUD, A. & TRYGGVASON, K. 2008. Laminin-511 but not -332, -111, or -411 enables mouse embryonic stem cell self-renewal in vitro. *Stem Cells,* 26, 2800-9.
DUVAL, K., GROVER, H., HAN, L. H., MOU, Y., PEGORARO, A. F., FREDBERG, J. & CHEN, Z. 2017. Modeling Physiological Events in 2D vs. 3D Cell Culture. *Physiology (Bethesda),* 32, 266-277.
ELLIS, S. J. & TANENTZAPF, G. 2010. Integrin-mediated adhesion and stem-cell-niche interactions. *Cell Tissue Res,* 339, 121-30.
ENGLER, A. J., CARAG-KRIEGER, C., JOHNSON, C. P., RAAB, M., TANG, H. Y., SPEICHER, D. W., SANGER, J. W., SANGER, J. M. & DISCHER, D. E. 2008. Embryonic cardiomyocytes beat best on a matrix with heart-like elasticity: scar-like rigidity inhibits beating. *J Cell Sci,* 121, 3794-802.
ENGLER, A. J., SEN, S., SWEENEY, H. L. & DISCHER, D. E. 2006. Matrix elasticity directs stem cell lineage specification. *Cell,* 126, 677-89.
ERTZEID, G. & STORENG, R. 2001a. The impact of ovarian stimulation on implantation and fetal development in mice. *Human reproduction,* 16, 221-5.
ERTZEID, G. & STORENG, R. 2001b. The impact of ovarian stimulation on implantation and fetal development in mice. *Hum Reprod,* 16, 221-5.
EVANS, M. J. & KAUFMAN, M. H. 1981. Establishment in culture of pluripotential cells from mouse embryos. *Nature,* 292, 154-6.
EVEN-RAM, S. & YAMADA, K. M. 2005. Cell migration in 3D matrix. *Curr Opin Cell Biol,* 17, 524-32.
FADINI, G. P., CICILIOT, S. & ALBIERO, M. 2017. Concise Review: Perspectives and Clinical Implications of Bone Marrow and Circulating Stem Cell Defects in Diabetes. *Stem Cells,* 35, 106-116.
FENG, G., JIN, X., HU, J., MA, H., GUPTE, M. J., LIU, H. & MA, P. X. 2011. Effects of hypoxias and scaffold architecture on rabbit mesenchymal stem cell differentiation towards a nucleus pulposus-like phenotype. *Biomaterials,* 32, 8182-9.
FRANTZ, C., STEWART, K. M. & WEAVER, V. M. 2010. The extracellular matrix at a glance. *J Cell Sci,* 123, 4195-200.
FRASER, J., WULUR, I., ALFONSO, Z., ZHU, M. & WHEELER, E. 2007. Differences in stem and progenitor cell yield in different subcutaneous adipose tissue depots. *Cytotherapy,* 9, 459-67.
GATES, A. H. & BOZARTH, J. L. 1978. Ovulation in the PMSG-treated immature mouse: effect of dose, age, weight, puberty, season and strain (BALB/c, 129 and C129F1 hybrid). *Biology of reproduction,* 18, 497-505.
GEORGES, P. C., MILLER, W. J., MEANEY, D. F., SAWYER, E. S. & JANMEY, P. A. 2006. Matrices with compliance comparable to that of brain tissue select neuronal over glial growth in mixed cortical cultures. *Biophys J,* 90, 3012-8.
GIANCOTTI, F. G. & RUOSLAHTI, E. 1999. Integrin signaling. *Science,* 285, 1028-32.
GINIS, I., LUO, Y., MIURA, T., THIES, S., BRANDENBERGER, R.,

GERECHT-NIR, S., AMIT, M., HOKE, A., CARPENTER, M. K., ITSKOVITZ-ELDOR, J. & RAO, M. S. 2004. Differences between human and mouse embryonic stem cells. *Dev Biol,* 269, 360-80.

GONG, S. P., KIM, H., LEE, E. J., LEE, S. T., MOON, S., LEE, H. J. & LIM, J. M. 2009. Change in gene expression of mouse embryonic stem cells derived from parthenogenetic activation. *Hum Reprod,* 24, 805-14.

GRIFFITH, L. G. & SWARTZ, M. A. 2006. Capturing complex 3D tissue physiology in vitro. *Nat Rev Mol Cell Biol,* 7, 211-24.

HANDSCHEL, J., NAUJOKS, C., DEPPRICH, R., LAMMERS, L., KUBLER, N., MEYER, U. & WIESMANN, H. P. 2011. Embryonic stem cells in scaffold-free three-dimensional cell culture: osteogenic differentiation and bone generation. *Head Face Med,* 7, 12.

HASS, R., KASPER, C., BOHM, S. & JACOBS, R. 2011. Different populations and sources of human mesenchymal stem cells (MSC): A comparison of adult and neonatal tissue-derived MSC. *Cell Commun Signal,* 9, 12.

HAUSCHKA, S. D. & KONIGSBERG, I. R. 1966. The influence of collagen on the development of muscle clones. *Proc Natl Acad Sci U S A,* 55, 119-26.

HAYASHI, Y., FURUE, M. K., OKAMOTO, T., OHNUMA, K., MYOISHI, Y., FUKUHARA, Y., ABE, T., SATO, J. D., HATA, R. & ASASHIMA, M. 2007. Integrins regulate mouse embryonic stem cell self-renewal. *Stem Cells,* 25, 3005-15.

HEYDARKHAN-HAGVALL, S., GLUCK, J. M., DELMAN, C., JUNG, M., EHSANI, N., FULL, S. & SHEMIN, R. J. 2012. The effect of vitronectin on the differentiation of embryonic stem cells in a 3D culture system. *Biomaterials,* 33, 2032-40.

HOFFMAN, L. M. & CARPENTER, M. K. 2005. Characterization and culture of human embryonic stem cells. *Nat Biotechnol,* 23, 699-708.

HUANG, X. Z., WU, J. F., CASS, D., ERLE, D. J., CORRY, D., YOUNG, S. G., FARESE, R. V., JR. & SHEPPARD, D. 1996. Inactivation of the integrin beta 6 subunit gene reveals a role of epithelial integrins in regulating inflammation in the lung and skin. *J Cell Biol,* 133, 921-8.

JANG, M., LEE, S. T., KIM, J. W., YANG, J. H., YOON, J. K., PARK, J. C., RYOO, H. M., VAN DER VLIES, A. J., AHN, J. Y., HUBBELL, J. A., SONG, Y. S., LEE, G. & LIM, J. M. 2013. A feeder-free, defined three-dimensional polyethylene glycol-based extracellular matrix niche for culture of human embryonic stem cells. *Biomaterials,* 34, 3571-80.

JENNINGS, H. S. 1911. "Genotype" and "Pure Line". *Science,* 34, 841-2.

JOHANNSEN, W. 2014. The genotype conception of heredity. 1911. *Int J Epidemiol,* 43, 989-1000.

JOHNSON, L. W., MOFFATT, R. J., BARTOL, F. F. & PINKERT, C. A. 1996. Optimization of embryo transfer protocols for mice. *Theriogenology,* 46, 1267-76.

JONES, R. G., LI, X., GRAY, P. D., KUANG, J., CLAYTON, F., SAMOWITZ, W. S., MADISON, B. B., GUMUCIO, D. L. & KUWADA, S. K. 2006. Conditional deletion of beta1 integrins in the intestinal epithelium causes a loss of Hedgehog expression, intestinal hyperplasia, and

early postnatal lethality. *J Cell Biol,* 175, 505-14.
KAINI, R. R., SHEN-GUNTHER, J., CLELAND, J. M., GREENE, W. A. & WANG, H. C. 2016. Recombinant Xeno-Free Vitronectin Supports Self-Renewal and Pluripotency in Protein-Induced Pluripotent Stem Cells. *Tissue Eng Part C Methods*.
KANG, Y., GEORGIOU, A. I., MACFARLANE, R. J., KLONTZAS, M. E., HELIOTIS, M., TSIRIDIS, E. & MANTALARIS, A. 2015. Fibronectin stimulates the osteogenic differentiation of murine embryonic stem cells. *J Tissue Eng Regen Med,* 11, 1929-1940.
KANIA, G., CORBEIL, D., FUCHS, J., TARASOV, K. V., BLYSZCZUK, P., HUTTNER, W. B., BOHELER, K. R. & WOBUS, A. M. 2005. Somatic stem cell marker prominin-1/CD133 is expressed in embryonic stem cell-derived progenitors. *Stem Cells,* 23, 791-804.
KELLER, G. M. 1995. In vitro differentiation of embryonic stem cells. *Curr Opin Cell Biol,* 7, 862-9.
KERN, S., EICHLER, H., STOEVE, J., KLUTER, H. & BIEBACK, K. 2006. Comparative analysis of mesenchymal stem cells from bone marrow, umbilical cord blood, or adipose tissue. *Stem Cells,* 24, 1294-301.
KINGWELL, K. 2013. Parkinson disease: Overcoming hurdles to stem-cell transplantation for treatment of Parkinson disease. *Nat Rev Neurol,* 9, 60.
LANE, S. W., WILLIAMS, D. A. & WATT, F. M. 2014. Modulating the stem cell niche for tissue regeneration. *Nat Biotechnol,* 32, 795-803.
LEAHY, A., XIONG, J. W., KUHNERT, F. & STUHLMANN, H. 1999. Use of developmental marker genes to define temporal and spatial patterns of differentiation during embryoid body formation. *J Exp Zool,* 284, 67-81.
LEE, M., AHN, J. I., AHN, J. Y., YANG, W. S., HUBBELL, J. A., LIM, J. M. & LEE, S. T. 2016. Difference in suitable mechanical properties of three-dimensional, synthetic scaffolds for self-renewing mouse embryonic stem cells of different genetic backgrounds. *J Biomed Mater Res B Appl Biomater*.
LEE, S. T., CHOI, M. H., LEE, E. J., GONG, S. P., JANG, M., PARK, S. H., JEE, H., KIM, D. Y., HAN, J. Y. & LIM, J. M. 2008. Establishment of autologous embryonic stem cells derived from preantral follicle culture and oocyte parthenogenesis. *Fertil Steril,* 90, 1910-20.
LEE, S. T., YUN, J. I., JO, Y. S., MOCHIZUKI, M., VAN DER VLIES, A. J., KONTOS, S., IHM, J. E., LIM, J. M. & HUBBELL, J. A. 2010. Engineering integrin signaling for promoting embryonic stem cell self-renewal in a precisely defined niche. *Biomaterials,* 31, 1219-26.
LEE, S. T., YUN, J. I., VAN DER VLIES, A. J., KONTOS, S., JANG, M., GONG, S. P., KIM, D. Y., LIM, J. M. & HUBBELL, J. A. 2012. Long-term maintenance of mouse embryonic stem cell pluripotency by manipulating integrin signaling within 3D scaffolds without active Stat3. *Biomaterials,* 33, 8934-42.
LEGGE, M. & SELLENS, M. H. 1994. Optimization of superovulation in the reproductively mature mouse. *Journal of assisted reproduction and genetics,* 11, 312-8.

LEHNER, B. 2013. Genotype to phenotype: lessons from model organisms for human genetics. *Nat Rev Genet,* 14, 168-78.
LEI, Y. & SCHAFFER, D. V. 2013. A fully defined and scalable 3D culture system for human pluripotent stem cell expansion and differentiation. *Proc Natl Acad Sci U S A,* 110, E5039-48.
LEONE, D. P., RELVAS, J. B., CAMPOS, L. S., HEMMI, S., BRAKEBUSCH, C., FASSLER, R., FFRENCH-CONSTANT, C. & SUTER, U. 2005. Regulation of neural progenitor proliferation and survival by beta1 integrins. *J Cell Sci,* 118, 2589-99.
LEVESQUE, J. P., TAKAMATSU, Y., NILSSON, S. K., HAYLOCK, D. N. & SIMMONS, P. J. 2001. Vascular cell adhesion molecule-1 (CD106) is cleaved by neutrophil proteases in the bone marrow following hematopoietic progenitor cell mobilization by granulocyte colony-stimulating factor. *Blood,* 98, 1289-97.
LI, C., YANG, Y., LU, X., SUN, Y., GU, J., FENG, Y. & JIN, Y. 2010. Efficient derivation of Chinese human embryonic stem cell lines from frozen embryos. *In Vitro Cell Dev Biol Anim,* 46, 186-91.
LI, S., HARRISON, D., CARBONETTO, S., FASSLER, R., SMYTH, N., EDGAR, D. & YURCHENCO, P. D. 2002. Matrix assembly, regulation, and survival functions of laminin and its receptors in embryonic stem cell differentiation. *J Cell Biol,* 157, 1279-90.
LIU, J., HUANG, J., LIN, T., ZHANG, C. & YIN, X. 2009. Cell-to-cell contact induces human adipose tissue-derived stromal cells to differentiate into urothelium-like cells in vitro. *Biochem Biophys Res Commun,* 390, 931-6.
LU, B. & ATALA, A. 2014. Small molecules and small molecule drugs in regenerative medicine. *Drug Discov Today,* 19, 801-8.
LUTOLF, M. P. & HUBBELL, J. A. 2003. Synthesis and physicochemical characterization of end-linked poly(ethylene glycol)-co-peptide hydrogels formed by Michael-type addition. *Biomacromolecules,* 4, 713-22.
LUTOLF, M. P., TIRELLI, N., CERRITELLI, S., CAVALLI, L. & HUBBELL, J. A. 2001. Systematic modulation of Michael-type reactivity of thiols through the use of charged amino acids. *Bioconjug Chem,* 12, 1051-6.
MARIANI, E. & FACCHINI, A. 2012. Clinical applications and biosafety of human adult mesenchymal stem cells. *Curr Pharm Des,* 18, 1821-45.
MARTIN, G. R. 1981. Isolation of a pluripotent cell line from early mouse embryos cultured in medium conditioned by teratocarcinoma stem cells. *Proc Natl Acad Sci U S A,* 78, 7634-8.
MARTINO, M. M., MOCHIZUKI, M., ROTHENFLUH, D. A., REMPEL, S. A., HUBBELL, J. A. & BARKER, T. H. 2009. Controlling integrin specificity and stem cell differentiation in 2D and 3D environments through regulation of fibronectin domain stability. *Biomaterials,* 30, 1089-97.
MCGEE, E. A. & HSUEH, A. J. 2000. Initial and cyclic recruitment of ovarian follicles. *Endocr Rev,* 21, 200-14.
MCWHIR, J., SCHNIEKE, A. E., ANSELL, R., WALLACE, H., COLMAN, A.,

SCOTT, A. R. & KIND, A. J. 1996. Selective ablation of differentiated cells permits isolation of embryonic stem cell lines from murine embryos with a non-permissive genetic background. *Nat Genet,* 14, 223-6.

MIAO, Y. L., KIKUCHI, K., SUN, Q. Y. & SCHATTEN, H. 2009. Oocyte aging: cellular and molecular changes, developmental potential and reversal possibility. *Human reproduction update,* 15, 573-85.

NARIAI, K., ISHINAZAKA, T., SUZUKI, K., UCHIYAMA, H., SATO, K., ASANO, R., TSUMAGARI, S., YUKAWA, M. & KANAYAMA, K. 2005. Optimum dose of LH-RH analogue Fertirelin Acetate for the induction of superovulation in mice. *Exp Anim,* 54, 97-9.

NIWA, H., MIYAZAKI, J. & SMITH, A. G. 2000. Quantitative expression of Oct-3/4 defines differentiation, dedifferentiation or self-renewal of ES cells. *Nat Genet,* 24, 372-6.

OKA, M., TAGOKU, K., RUSSELL, T. L., NAKANO, Y., HAMAZAKI, T., MEYER, E. M., YOKOTA, T. & TERADA, N. 2002. CD9 is associated with leukemia inhibitory factor-mediated maintenance of embryonic stem cells. *Mol Biol Cell,* 13, 1274-81.

PAMPALONI, F., REYNAUD, E. G. & STELZER, E. H. 2007. The third dimension bridges the gap between cell culture and live tissue. *Nat Rev Mol Cell Biol,* 8, 839-45.

PAREKKADAN, B. & MILWID, J. M. 2010. Mesenchymal stem cells as therapeutics. *Annu Rev Biomed Eng,* 12, 87-117.

PARK, H. J., LEE, P. H., BANG, O. Y., LEE, G. & AHN, Y. H. 2008. Mesenchymal stem cells therapy exerts neuroprotection in a progressive animal model of Parkinson's disease. *J Neurochem,* 107, 141-51.

POTAPOVA, I. A., BRINK, P. R., COHEN, I. S. & DORONIN, S. V. 2008. Culturing of human mesenchymal stem cells as three-dimensional aggregates induces functional expression of CXCR4 that regulates adhesion to endothelial cells. *J Biol Chem,* 283, 13100-7.

PROWSE, A. B., CHONG, F., GRAY, P. P. & MUNRO, T. P. 2011. Stem cell integrins: implications for ex-vivo culture and cellular therapies. *Stem Cell Res,* 6, 1-12.

PRZYBORSKI, S. A. 2005. Differentiation of human embryonic stem cells after transplantation in immune-deficient mice. *Stem Cells,* 23, 1242-50.

RAYMOND, K., DEUGNIER, M. A., FARALDO, M. M. & GLUKHOVA, M. A. 2009. Adhesion within the stem cell niches. *Curr Opin Cell Biol,* 21, 623-9.

SABAGHI, F., SHAMSASENJAN, K., MOVASAGHPOUR, A. A., AMIRIZADEH, N., NIKOUGOFTAR, M. & BAGHERI, N. 2016. Evaluation of human cord blood CD34+ hematopoietic stem cell differentiation to megakaryocyte on aminated PES nanofiber scaffold compare to 2-D culture system. *Artif Cells Nanomed Biotechnol,* 44, 1062-8.

SCHOLER, H. R., RUPPERT, S., SUZUKI, N., CHOWDHURY, K. & GRUSS, P. 1990. New type of POU domain in germ line-specific protein Oct-4. *Nature,* 344, 435-9.

SENSEBE, L., KRAMPERA, M., SCHREZENMEIER, H., BOURIN, P. & GIORDANO, R. 2010. Mesenchymal stem cells for clinical application. *Vox Sang,* 98, 93-107.

SHEN, Q., WANG, Y., KOKOVAY, E., LIN, G., CHUANG, S. M., GODERIE, S. K., ROYSAM, B. & TEMPLE, S. 2008. Adult SVZ stem cells lie in a vascular niche: a quantitative analysis of niche cell-cell interactions. *Cell Stem Cell,* 3, 289-300.

SIMPSON, E. M., LINDER, C. C., SARGENT, E. E., DAVISSON, M. T., MOBRAATEN, L. E. & SHARP, J. J. 1997. Genetic variation among 129 substrains and its importance for targeted mutagenesis in mice. *Nat Genet,* 16, 19-27.

SOLTER, D. & KNOWLES, B. B. 1978. Monoclonal antibody defining a stage-specific mouse embryonic antigen (SSEA-1). *Proc Natl Acad Sci U S A,* 75, 5565-9.

SUZUKI, O., ASANO, T., YAMAMOTO, Y., TAKANO, K. & KOURA, M. 1996. Development in vitro of preimplantation embryos from 55 mouse strains. *Reproduction, fertility, and development,* 8, 975-80.

SWIFT, J., IVANOVSKA, I. L., BUXBOIM, A., HARADA, T., DINGAL, P. C., PINTER, J., PAJEROWSKI, J. D., SPINLER, K. R., SHIN, J. W., TEWARI, M., REHFELDT, F., SPEICHER, D. W. & DISCHER, D. E. 2013. Nuclear lamin-A scales with tissue stiffness and enhances matrix-directed differentiation. *Science,* 341, 1240104.

TANIGUCHI, M., GUAN, L. L., ZHANG, B., DODSON, M. V., OKINE, E. & MOORE, S. S. 2008. Adipogenesis of bovine perimuscular preadipocytes. *Biochem Biophys Res Commun,* 366, 54-9.

TARIN, J. J., PEREZ-ALBALA, S. & CANO, A. 2001. Cellular and morphological traits of oocytes retrieved from aging mice after exogenous ovarian stimulation. *Biology of reproduction,* 65, 141-50.

TE VELDE, E. R. & PEARSON, P. L. 2002. The variability of female reproductive ageing. *Human reproduction update,* 8, 141-54.

THOMSON, J. A., ITSKOVITZ-ELDOR, J., SHAPIRO, S. S., WAKNITZ, M. A., SWIERGIEL, J. J., MARSHALL, V. S. & JONES, J. M. 1998. Embryonic stem cell lines derived from human blastocysts. *Science,* 282, 1145-7.

VAN DER AUWERA, I. & D'HOOGHE, T. 2001. Superovulation of female mice delays embryonic and fetal development. *Human reproduction,* 16, 1237-43.

VEEVERS-LOWE, J., BALL, S. G., SHUTTLEWORTH, A. & KIELTY, C. M. 2011. Mesenchymal stem cell migration is regulated by fibronectin through alpha5beta1-integrin-mediated activation of PDGFR-beta and potentiation of growth factor signals. *J Cell Sci,* 124, 1288-300.

VITILLO, L., BAXTER, M., ISKENDER, B., WHITING, P. & KIMBER, S. J. 2016. Integrin-Associated Focal Adhesion Kinase Protects Human Embryonic Stem Cells from Apoptosis, Detachment, and Differentiation. *Stem Cell Reports,* 7, 167-76.

WAGNER, W., WEIN, F., SECKINGER, A., FRANKHAUSER, M., WIRKNER, U., KRAUSE, U., BLAKE, J., SCHWAGER, C., ECKSTEIN, V., ANSORGE, W. & HO, A. D. 2005. Comparative characteristics of

mesenchymal stem cells from human bone marrow, adipose tissue, and umbilical cord blood. *Exp Hematol,* 33, 1402-16.

WAJCHENBERG, B. L. 2000. Subcutaneous and visceral adipose tissue: their relation to the metabolic syndrome. *Endocr Rev,* 21, 697-738.

WOBUS, A. M., KIESSLING, U., STRAUSS, M., HOLZHAUSEN, H. & SCHONEICH, J. 1984. DNA transformation of a pluripotent mouse embryonal stem cell line with a dominant selective marker. *Cell Differ,* 15, 93-7.

WOZNIAK, M. A., MODZELEWSKA, K., KWONG, L. & KEELY, P. J. 2004. Focal adhesion regulation of cell behavior. *Biochim Biophys Acta,* 1692, 103-19.

XIE, T. & SPRADLING, A. C. 2000. A niche maintaining germ line stem cells in the Drosophila ovary. *Science,* 290, 328-30.

YING, Q. L., NICHOLS, J., CHAMBERS, I. & SMITH, A. 2003. BMP induction of Id proteins suppresses differentiation and sustains embryonic stem cell self-renewal in collaboration with STAT3. *Cell,* 115, 281-92.

ZARROW, M. X. & WILSON, E. D. 1961. The influence of age on superovulation in the immature rat and mouse. *Endocrinology,* 69, 851-5.

ZHU, A. J., HAASE, I. & WATT, F. M. 1999. Signaling via beta1 integrins and mitogen-activated protein kinase determines human epidermal stem cell fate in vitro. *Proc Natl Acad Sci U S A,* 96, 6728-33.

ZUK, P. A., ZHU, M., ASHJIAN, P., DE UGARTE, D. A., HUANG, J. I., MIZUNO, H., ALFONSO, Z. C., FRASER, J. K., BENHAIM, P. & HEDRICK, M. H. 2002. Human adipose tissue is a source of multipotent stem cells. *Mol Biol Cell,* 13, 4279-95.

SUMMARY IN KOREAN

본 연구의 목표는 연구 목표는 마우스와 인간에서 줄기세포를 확보하고 그에 적합한 배양 미세환경을 개발하는 것이다. 먼저 마우스와 인간에서 줄기세포를 채취, 확립하는 방법에 대한 연구를 진행한 후 줄기세포의 표면 인테그린 정보에 대한 조사를 실시하였다.

그 이후 세포의 배양에 적합한 조건의 배양환경을 3D 구조로 개발하였다.

줄기세포는 생체 내에서는 삼차원적인 조건에서 존재하는 데 현재 연구환경에서는 주로 2차원적 환경에서 배양이 이루어지고 있다. 이에 본 연구는 세포의 삼차원적 배양환경을 연구실에서 구축함으로서 세포의 삼차원적 배양환경을 모사하는 데에 초점을 두었다.

본 연구에서는 세포에 따른 비세포성 미세환경적 변화가 필요할 것이라고 가정하고 실험을 진행하였으며 이에 그 성질이 비슷하지만 그 유전적 기원이 다른 두 마우스 배아줄기세포와 확연히 그 특성이 다른 인간지방 유래 기질세포에 각각 적합한 구성의 미세환경을 구현하였다.

결과적으로 세포의 배경, 특성에 따라 세포에 적합한 생체유사 미세환경이 다름을 확인할 수 있었으며 차후에 다른 세포에 적합한 배양 미세환경을 조성할 필요가 있을 시 본 연구가 보탬이 될 것을 기대한다.